



Contents lists available at ScienceDirect

Expert Systems With Applications

journal homepage: www.elsevier.com/locate/eswa

Gait monitoring system for patients with Parkinson's disease

Helena R. Gonçalves^{a,*}, Ana Rodrigues^b, Cristina P. Santos^a^a University of Minho, Center for MicroElectroMechanical, Portugal^b Hospital of Braga, Neurology Service, Portugal

ARTICLE INFO

Keywords:

Wearable sensors
Adaptive computational method
Real-time application
Gait monitoring system
Parkinson's disease

ABSTRACT

Background: Wearable monitoring devices based on inertial sensors have the potential to be used as a quantitative method in clinical practice for continuous assessment of gait disabilities in Parkinson's disease (PD).

Methods: This manuscript introduces a new gait monitoring system adapted to patients with PD, based on a wearable monitoring device. To eliminate inter- and intra-subject variability, the computational method was based on heuristic rules with adaptive thresholds and ranges and a motion compensation strategy. The experimental trials involved repeated measurements of walking trials from two cross-sectional studies: the first study was performed in order to validate the effectiveness of the system against a robust 3D motion analysis with 10 healthy subjects; and the second-one aimed to validate our approach against a well-studied wearable IMU-based system on a hospital environment with 20 patients with PD.

Results: The proposed system proved to be efficient (Experiment I: sensitivity = 95,09% and accuracy = 93,64%; Experiment II: sensitivity = 99,53% and accuracy = 97,42%), time-effective (Experiment I: earlies = 13,71 ms and delays = 12,91 ms; Experiment II: earlies = 12,94 ms and delays = 12,71 ms), user and user-motion adaptable and a low computational-load strategy for real-time gait events detection. Further, it was measured the percentage of absolute error classified with a good acceptability (Experiment I: $3,02 \leq \epsilon\% \leq 12,94$; Experiment II: $2,81 \leq \epsilon\% \leq 13,45$). Lastly, regarding the measured gait parameters, it was observed a reflection of the typical levels of motor impairment for the different disease stages.

Conclusion: The achieved outcomes enabled to verify that the proposed system can be suitable for gait analysis in the assistance and rehabilitation fields.

1. Introduction

Monitoring gait disabilities frequently observed in Parkinson's disease (PD) is difficult for clinicians, as they are limited to the information observed or self-reported during the routine-consultations, resulting in subjectivity and limited assessment (Dijkstra, Zijlstra, Scherder, & Kamsma, 2008; Moore, Dilda, Hakim, & MacDougall, 2011). It is required to increase the frequency of assessment, including more often (out of routine consultations) and/or objectively (avoiding subjects' recall of memory). Continuous spatiotemporal gait parameters analysis enables to monitor individualized motor performance changes during the course of the disease (Del Din, Godfrey, & Rochester, 2016; Dijkstra et al., 2008; Link et al., 2009; Moore et al., 2011; Patel et al., 2007). Consequently, tracking patients' gait behavior could constitute a biomarker of illness stage, allowing to adopt personalized treatments and consequently delaying patients' motor symptoms (Del Din, Godfrey, & Rochester, 2016; Dijkstra et al., 2008; Link et al., 2009; Moore et al.,

2011; Patel et al., 2007). However, there is still no ambulatory system that allows clinicians to access this information reliably (Pistacchi et al., 2017). It is needed to find devices and algorithms which are able to provide a continuous gait assessment and allow an assessment more oriented to daily motor tasks, as cited by Maetzler, Domingos, Srulijes, Ferreira, & Bloem, 2013 and Iijima & Takahashi, 2020.

Research has focused in new monitoring and assessment technologies based on video-based motion camera systems, robotic systems, and virtual reality applications (Godinho et al., 2016). However, these solutions are often very costly, limiting their use in clinical settings, regardless of their effectiveness (Godinho et al., 2016; Schlachetzki, Barth, Marxreiter, Gossler, Kohl, Reinfelder, & Klucken, 2017; Suzuki, Mitoma, & Yoneyama, 2017; Zago et al., 2018). Given the mass use of smartphones, the number of smart applications for motor monitoring in PD increased over the last years (Linares-del Rey, Vela-Desojo, & Cano-de la Cuerda, 2019). Advances included to monitor speech and tremor besides to provide gait analysis (Palacios-Alonso et al., 2020).

* Corresponding author at: Center for MicroElectroMechanical, University of Minho – Azurém Campus, 4800-058 Guimarães, Portugal.

E-mail addresses: id7609@alunos.uminho.pt (H.R. Gonçalves), crisrina@dei.uminho.pt (C.P. Santos).

<https://doi.org/10.1016/j.eswa.2021.115653>

Received 20 February 2021; Received in revised form 21 June 2021; Accepted 21 July 2021

Available online 26 July 2021

0957-4174/© 2021 Elsevier Ltd. All rights reserved.

Nevertheless, scientific evidence of their usefulness is limited and of poor quality and further studies are required to validate these tools and customize their use, as indicated in review (Linares-del Rey et al., 2019).

Recent advances in body-worn sensors enabled a continuous gait assessment and availability in domiciliary scenarios. Inertial measurement units (IMUs) have been successfully used to measure mobility and provide a cost-effective and lightweight solution for comprehensive gait assessment in laboratory, clinical, and community environments. Even though inertial sensors are not still routinely used for diagnosis of PD or treatment assessment purposes (Rastegari, Azizian, & Ali, 2019), they have already been used to investigate motor complications in PD as in (Beck et al., 2018; Del Din, Godfrey, & Rochester, 2016; Del Din, Godfrey, Galna, Lord, & Rochester, 2016; Hundza et al., 2014; Lipsmeier et al., 2018; Morris et al., 2019; Okuda et al., 2016; Rastegari et al., 2019; Schlachetzki et al., 2017; Zago et al., 2018). Progression in commercial IMUs development has led to novel algorithms for gait events detection based on inertial data processing (Alvarez, Lo, Rodriguez-uri, Diego, & Gonza, 2010; Beck et al., 2018; Del Din, Godfrey, & Rochester, 2016; Del Din, Godfrey, Galna et al., 2016; Gonçalves, Moreira, Rodrigues, Minas, Reis, & Santos, 2018; Hundza et al., 2014; Lipsmeier et al., 2018; Morris et al., 2019; Okuda et al., 2016; Schlachetzki et al., 2017; Trojaniello, Ravaschio, Hausdorff, & Cereatti, 2015; Zago et al., 2018).

Lower trunk inertial signals processing is an efficient solution when it is intended to segment the human gait, using just one inertial sensor without requiring large processing requirements, and enhance the opportunity to apply the system during the patients' daily walking tasks (Alvarez et al., 2010; Gonçalves et al., 2018; McCamley, Donati, Grim-pampi, & Mazzà, 2012; Menz, Lord, & Fitzpatrick, 2003; Okuda et al., 2016; Trojaniello et al., 2014, 2015). A previous study accomplished by our team (Gonçalves et al., 2018) enabled to detect in real-time five gait cycles - Heel-strike (HS), Foot-flat (FF), Toe-off (TO), Mid-stance (MSt) and Heel-off (HO) - with an accuracy varying between 93.94 and 99.98% and earlier/delays of 2.17–11.8 ms, in healthy subjects through the analysis of the vertical acceleration of the lower trunk, using a finite state machine (FSM) computational method. To the best knowledge of the authors, no study in the literature has already validated a real-time and versatile threshold-based FSM for gait segmentation from lower trunk acceleration particularly with patients with PD (Alvarez et al., 2010; Gonçalves et al., 2018; Trojaniello et al., 2015). Furthermore, systems' development needs benchmarking validation against robust and previously validated systems, before being implemented in clinical settings (Morris et al., 2019). Morris et al., 2019 and Zago et al., 2018 compared an IMU-based wearable system against an instrumented walkway and an optoelectronic system, respectively, obtaining relevant results with PD patients. However, they performed the experimental tests in controlled environments and based on simple walking tests, *i.e.* without velocity variations or inclusion of other walking scenarios (Morris et al., 2019; Zago et al., 2018).

Computational methods based on machine learning are another approach that has been heavily explored to recognize patterns in patients' gait (Beck et al., 2018; Brognara, Palumbo, Grimm, & Palmerini, 2019; Caramia et al., 2018; Rastegari et al., 2019). However, this approach demands high computational power and memory requirements, being not feasible for real-time applications (Brognara et al., 2019), besides to be frequently used for pathological gait classification and not for gait events segmentation (Beck et al., 2018; Brognara et al., 2019; Caramia et al., 2018; Rastegari et al., 2019). Real-time implementations are relevant for integration of the motion system with actuation systems to provide active motor assistance and thus producing high-aid technologies. Indeed, to mitigate gait-associated impairments in PD, patients may benefit from biofeedback devices that integrate a motion analysis system to collect, for instance, users' gait information and, in real-time, process acquired data and provide sensory cues accordingly (Sweeney et al., 2019).

A comprehensive and critical examination on previous gait

monitoring systems in PD field allows to identify some challenges that remain to fulfill, including: (i) limited and inconsistent implementations for outside laboratory conditions; (ii) critical validation of FSM-based computation methods with the end-users; (iii) limited computational solutions for real-time applications able to overcome inter/intra-subject variability; (iv) absence of automatic and adaptable systems to the patients' movement, *i.e.* providing motion compensation; and (v) further analysis between gait parameters and clinical scales associated to PD, as Hoehn & Yahr scale (H&Y) and Unified Parkinson's Disease Rating Scale (UPDRS) (Goetz et al., 2008; Hoehn & Yahr, 1967). In this sense, the purpose of this study was to take a systematic approach to address each of these challenges, holding three main goals.

First, this research aimed to implement a new gait monitoring system adapted to PD able to analyze patients' walking information continuously and objectively outside a laboratory context, in clinical environment. The system relies on the use of recent wearable technology to guarantee more freedom of movement to the patients, being able to be used in different situations. We present a compact system, based on the use of an IMU located in L5 to acquire inertial information. The main challenge was the integration of the inertial acquisition system on a single wearable device and the development of a real-time, adaptable, and time-effective gait events detection algorithm. Based on a heuristic approach, an FSM with decision rules to gait characterization was implemented to detect five gait events (HS, FF, MSt, TO and HO). Considering the dynamic involved in real-life walk conditions, a motion compensation strategy and adaptive thresholds were adopted. Further, we estimated six promising spatiotemporal gait parameters: step/stride duration/length, velocity, and cadence. The second goal covered a benchmarking analysis against pre-validated commercial systems. The manuscript reports a continuous investigation along two main phases of experiments: firstly, it was verified the effectiveness of our gait analysis system against a robust 3D motion analysis based on Vicon® capture cameras with healthy subjects in a controlled environment; and then, on a clinical environment, at Hospital de Braga facilities, with patients with PD, our system was validated against a well-studied wearable IMU-based system, Xsens®. Gait parameters estimation allowed to compare the measured gait-associated metrics with the patients' PD stage, addressing the third goal. Thus, it was possible to analyze if the measured spatiotemporal gait parameters corresponded to the motor impairment characterized by the PD scales and to verify the hypothesis that motor function assessment may indicate a future "bio-mark" of patient stage. The proposed solution is expected to provide a customized system able to monitor patients' gait in a continuous and objective way, and to produce a modular motion system that could be integrated on actuation systems aiming to provide active assistance. Notwithstanding, neurologists will also benefit from this technology by receiving more complete information about their patients' locomotion state.

2. Materials and methods

2.1. Gait monitoring system requirements & set-up

Functional, operational and hardware requirements were identified for the proposed solution. For functional requirements, we identified that the system should enable time-effective and versatile gait events detection and provide gait parameters estimation. Regarding operational requirements, we defined that the system instrumentation should be fully integrated on a wearable device and include a user-friendly GUI able to wirelessly access the device and display the processed data. Hardware requirements include system ability to storage the acquired and processed data at 100 Hz, Bluetooth wireless network range of at least 8 m, a system autonomy of at least 8 h assisting prolonged recording, and electrical circuitry integrated into a miniaturized board and isolated from the user. The proposed Gait Monitoring System comprises five main HW-SW units: (1) Sensory Acquisition Unit, (2) Processing Unit, (3) Data Storage Unit, (4) Mobile APP and a (5) Desktop

GUI, as represented in Fig. 1.

Sensory Acquisition unit comprises a single IMU (MPU-6050) for acquiring inertial data, which includes an accelerometer and gyroscope from a unique sensor board. Data are recorded from both accelerometer and gyroscope sensors, with a full-scale range respectively of $\pm 4\text{ g}$ and $250^\circ/\text{s}$ (enough to detect gait events through a lower trunk acquisition) at a sampling frequency of 100 Hz. Processing unit receives and processes the acceleration and gyroscope data and runs the real-time gait events detection algorithm. It relies on a microcontroller Atmega 2560 suitable to establish the serial communication, I2C protocol and SPI bus between the other interfaces. A SD card is included to store the inertial data and the gait events detected in real-time (by saving the finite state machine states). Data processing and saving are also performed at a frequency of 100 Hz, which is enough to analyze a complete gait cycle. A Bluetooth module is used to communicate with an Android mobile APP, to wirelessly start/stop the trials and plot the acquired inertial data. The stored information in SD card is downloaded and, from the real-time detected gait events and inertial data, gait-associated parameters are estimated in a desktop GUI, created in MATLAB®. The use of front-edge, miniaturized, light and low power-consumption electronic technology allows the system to be fully integrated into a wearable device, an instrumented waistband. The presented HW-SW set-up enabled to fulfill the identified functional and operational requirements.

2.2. Gait events detection

The proposed gait events detection algorithm detects the HS, FF, MSt, TO and HO for each leg. Given that this algorithm was firstly developed for healthy adults, we named it as H-GED. The method consists of six stages: (1) calibration, (2) motion compensation, (3) filtering, (4) 1st derivative computation, (5) finite state machine and (6) thresholds and events range duration calculation. Both acceleration and angular velocity signals are used for the first two stages, whilst only the vertical acceleration is used for the next stages, as depicted in Fig. 2.

Calibration. For on-body calibration routine, 500 samples (acc_n and gyr_n) are captured, which are used to calculate an offset that is withdrawn from each of the samples subsequently acquired. This calibration allows to eliminate measurement error.

Motion compensation. Each gait event can be assigned to a specific peak in lower trunk inertial signals, which present constant waveforms during a complete gait cycle. However, such inertial signal waveforms are affected by the users' motion, like trunk rotations. Aiming to define common heuristic decision rules for gait events detection based on inertial signal waveforms, it is required to minimize any subjectivity introduced by those users' movements. This procedure is particularly

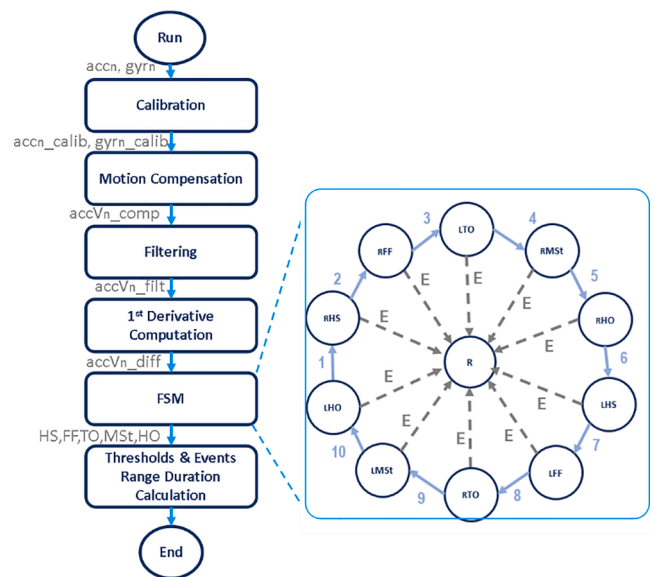


Fig. 2. Computational method for real-time gait events detection in healthy adults (H-GED): flowchart of the proposed gait monitoring system.

relevant for an application of gait monitoring in patients' home scenarios, which include different motor daily tasks and multitasking. We added a motion compensation strategy to reduce the impact of users' trunk movement besides their natural trunk motion during walking, aiming to ensure the constant waveforms of acquired inertial signals. Thus, calibrated acceleration and angular velocity samples (acc_n_{calib} and gyr_n_{calib}) are used to estimate the pitch and roll angles of lower trunk: the pitch angle corresponds to rotation of the trunk along the frontal plane, while the roll angle concerns to the trunk rotation along the sagittal plane. This estimation allows to align the acquired inertial signals with the conventional axis regardless the user motion and apply common decision rules. Pitch and roll angles estimation were based on Kalman Filter, as described in (Mccarron, 2013). Fig. 3 (middle panel) depicts an example of the motion compensation of the acceleration vertical signal (acc_n_{comp}) when a user executes a positive rotation of his/her trunk along the frontal plane. It is possible to verify that at the time of rotation, the acceleration signal was compensated.

Filtering. Compensated vertical acceleration samples are filtered ($accVn_{filt}$) by an exponential filter, which is ideal for real-time implementations, since it does not cause delays in the signal and smooths the

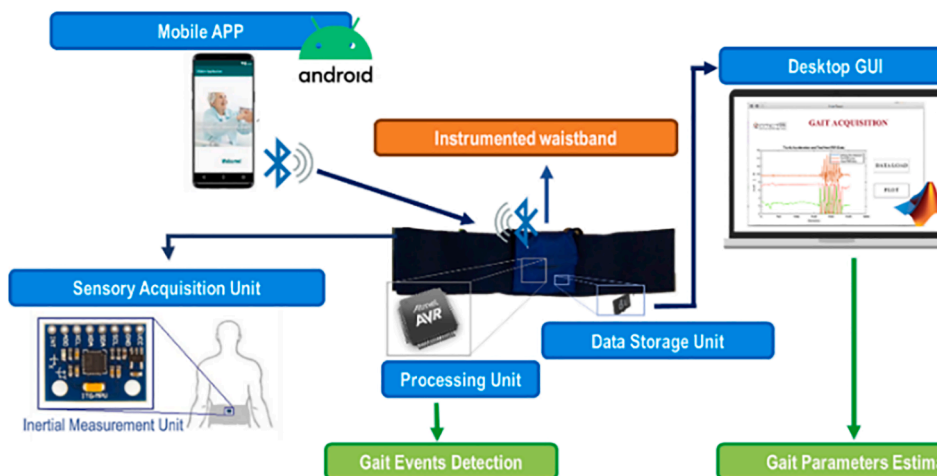


Fig. 1. Proposed gait monitoring system. HW/SW units (blue): (1) sensory acquisition unit, (2) processing unit and (3) data storage unit embedded in the waistband (orange); (4) mobile APP and (5) desktop GUI. System functionalities (green): gait events detection and gait parameters estimation.

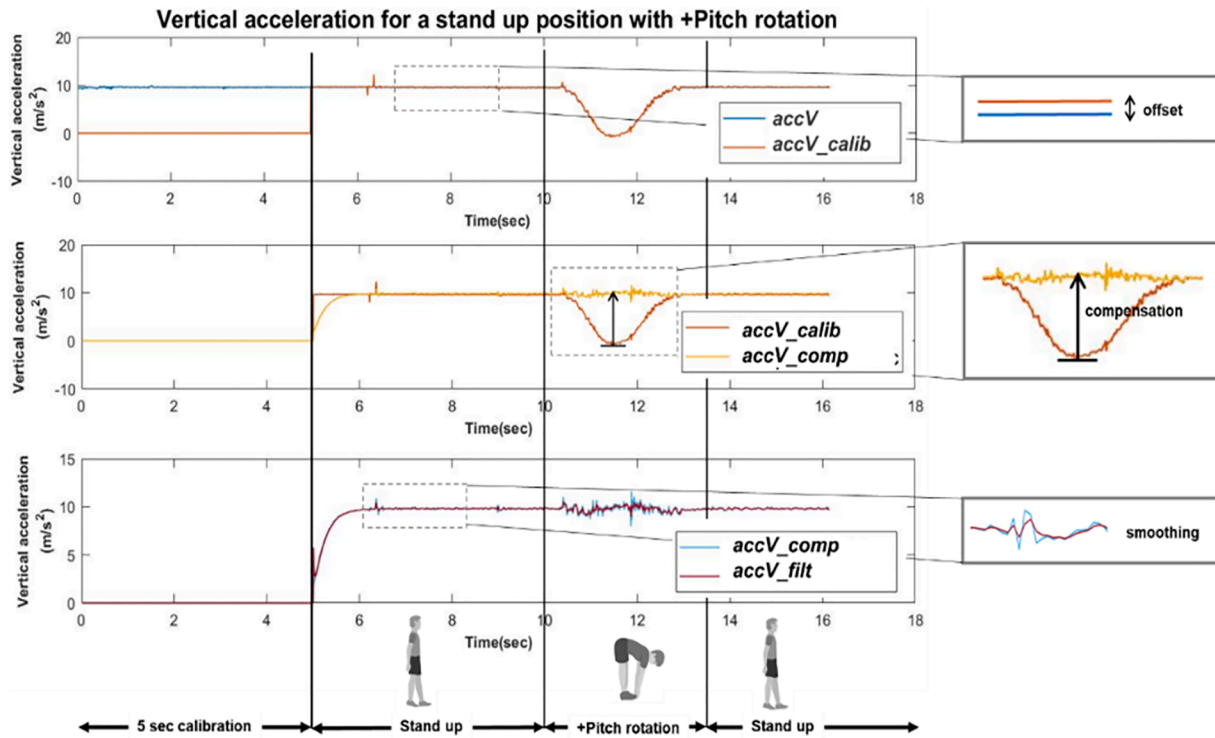


Fig. 3. Vertical acceleration along the phases of the proposed algorithm for a stand up position with positive pitch rotation: 5 s of calibration; 10 s in stand up position; approximately 3 s of positive trunk positive rotation; and return to the standup position. **Above:** raw and calibrated vertical acceleration ($accV$ and $accV_{calib}$); **Middle:** calibrated and compensated vertical acceleration ($accV_{calib}$ and $accV_{comp}$); **Below:** compensated vertical acceleration and filtered compensated vertical acceleration ($accV_{comp}$ and $accV_{filt}$).

signal. The smoothing factor of the filter was set to 0.5 by trial and error.

1st derivative computation. After filtering, the 1st derivative is determined ($accV_n_{diff}$) to detect when the acceleration increases, decreases, or remains constant. To deal with noise, the derivatives below a threshold (near to zero but empirically set) were assumed as null. This allows to detect only major variations, that usually are associated with local/global peaks, which can correspond to a gait event, as described in Fig. 4.A.

Finite state machine. We segment the vertical acceleration signal into five gait events for each leg (totalizing ten events), where each signal peak corresponds to a gait event in the constant waveform during a gait cycle (Fig. 4.A). For that, a FSM based on heuristic decision rules is implemented by means of a switch case statement, which changes between states in accordance with the decision rules presented in Table 1. We specified ten decision rules based on curve tracing techniques including the evaluation of signal derivatives ($accV_n_{diff}$) and adaptive thresholds ($th_{R/L_{HS}}$, $th_{R/L_{FF}}$, $th_{R/L_{TO}}$, $th_{R/L_{MSt}}$ and $th_{R/L_{HO}}$), as depicted in Fig. 4.B. Evaluation of signal derivatives allows to detect maximum and minimum peaks (maximum: $accV_n_{diff} < 0$ & $accV_{n-1}_{diff} > 0$; minimum: $accV_n_{diff} > 0$ & $accV_{n-1}_{diff} < 0$) and the use of thresholds eliminates unclear local peaks (maximum: $accV_n_{diff} > th$; minimum: $accV_n_{diff} < th$). We defined HS, FF and MSt as maximums, and TO and HO as minimums. Each decision rule presented allows to trigger from one event to the following. FSM is constituted by eleven states that correspond to ten gait events (five for each leg) and one for reset state.

Adaptive thresholds and events range duration calculation. Daily life walking situations, as climbing stairs or variations in gait speed affect the duration of a gait cycle and the amplitude of inertial signals. Traditional FSMs present a static behavior which do not address such gait patterns alterations during common human walking situations. To overcome this lack and based on our previous work (Figueiredo, Felix, Costa, Moreno, & Santos, 2018; Gonçalves et al., 2018), we added a versatile feature to the proposed FSM by using adaptive thresholds and

events range duration instead of static thresholds as typically used. Furthermore, this versatility can minimize redundancy from intra/inter-usability. The used thresholds in the FSM decision rules ($th_{R/L_{HS}}$, $th_{R/L_{FF}}$, $th_{R/L_{TO}}$, $th_{R/L_{MSt}}$ and $th_{R/L_{HO}}$) are adapted every five gait cycles ($count_{gait_cycle} = 5$) and defined as 80% of the mean value of the accelerations of the previous events detected ($acc_{R/L_{HS}}$, $acc_{R/L_{FF}}$, $acc_{R/L_{TO}}$, $acc_{R/L_{MSt}}$ and $acc_{R/L_{HO}}$) as depicted in Fig. 4.C. Also, after five gait cycles, gait events are detected based on previous event moments ($pos_{R/L_{HS}_{n-1}}$, $pos_{R/L_{FF}_{n-1}}$, $pos_{R/L_{TO}_{n-1}}$, $pos_{R/L_{MSt}_{n-1}}$ and $pos_{R/L_{HO}_{n-1}}$) and an adaptable estimated range between the previous and actual event moments ($range_{R/L_{HS}}$, $range_{R/L_{FF}}$, $range_{R/L_{TO}}$, $range_{R/L_{MSt}}$ and $range_{R/L_{HO}}$). This range is calculated every three gait cycles ($count_{gait_cycle} = 3$) and results as 80% of the mean difference between the moment of the current event and the previous gait event as indicated in Fig. 4.C. Initial values, percentages defined to update the adaptive thresholds and events duration range, as also the number of gait cycles to calculate these values, were empirically found after an exhaustive inspection of the vertical acceleration signal supported by previous work and respective findings for different users and walking conditions (Figueiredo et al., 2018; Gonçalves et al., 2018).

Motion compensation, filtering, 1st derivative computation and the adaptive decision rules depend on the current sample and on the previous sample acquired (acc_n , acc_{n-1} , gyr_n and gyr_{n-1}), so these values are always stored at the end of each cycle. For the first sample acquired, it is assumed that the previous sample is zero. Moreover, in order to assign an event to a leg, it was mandatory for the user to start walking with the right leg, as indicated in (Auvinet et al., 2002).

2.3. Gait events detection adapted to patients with PD

The proposed gait events detection algorithm after being validated with healthy subjects (H-GED) needed to be adapted to patients with PD (PD-GED) through the inclusion of some adaptations in the FSM. Further, we added the capability of distinguishing which leg was

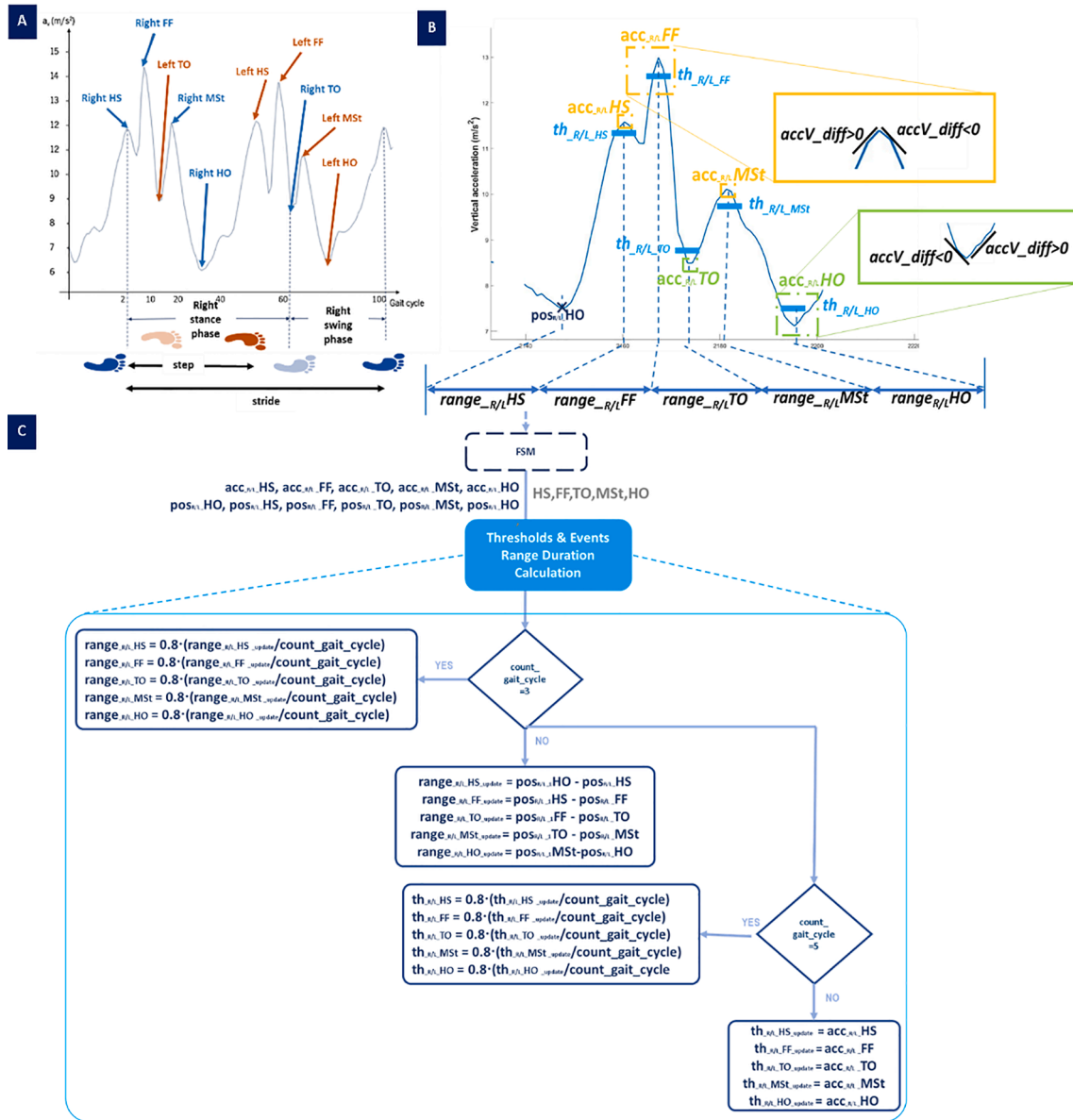


Fig. 4. **A:** Lower trunk vertical acceleration over one stride for a healthy subject. **B:** Adaptive thresholds, Events Range Duration and highlight for the derivative ($accV_diff$) behavior for a maximum detection (HS, FF and MSt) and for a minimum detection (TO and HO); **C:** Zoom-in flowchart stage Threshold & Events Range Duration Calculation of the proposed method.

performing an event without initial assumptions, as depicted in Fig. 5.

Finite state machine adapted to PD. PD patients have a different walking pattern, and thus it was necessary to adapt the FSM decision rules for gait events detection in PD. We verified from the first six patients, an absence or low prominence of the first local maximum which was used to determine the HS (Fig. 6). To overcome this alteration, the foot initial contact (HS) is instead defined as in (Auvinet et al., 2002), in which the HS corresponds to a global maximum in the acceleration signal in the anteroposterior plane. Therefore, we changed the adaptive decision rules to detect this peak in the anteroposterior plane, starting to consider the anteroposterior acceleration for the Motion Compensation ($accAP_n\ comp$), Filtering ($accAP_n\ filt$), and 1st Derivative Computation ($accAP_n\ diff$) phases. Force sensor resistors in soles of the patients allowed to confirm these alterations, as depicted in Fig. 6.A. As in H-GED computational method, FF, TO, MSt and HO correspond to maximum and minimum peaks on the vertical acceleration signal. Five decision rules were implemented to detect these gait events, that allow to trigger from one state to another, based on evaluation of signal derivatives

($accAP_n\ diff$ and $accV_n\ diff$) and adaptive thresholds (th_{HS} , th_{FF} , th_{TO} , th_{MSt} and th_{HO}) as indicated in Table 2.

Event-to-leg assigning. A new phase was added to the gait analysis algorithm to assign the detected event to the corresponding leg. The identification is based on the analysis of the angular velocity signal, as depicted in Fig. 6.B. When a HS event is detected, the signal of the gyroscope in antero-posterior plane ($gyrAP_n$) is analyzed: if this signal is positive, the corresponding leg which performed the HS gait event is the left one; but, if the signal is negative, the HS event is assigned to the right leg. When the right leg is assigned to a HS, except for the TO event, the following events (FF, MSt and HO) are assigned to the same leg (Alvarez et al., 2010; Auvinet et al., 2002). TO event corresponds to the leg opposite to the one identified in HS event as depicted in Fig. 6.A in accordance with what is described in (Alvarez et al., 2010; Auvinet et al., 2002). This alteration enabled to reduce the number of decision rules used in the H-GED and ensure that the detected event would be correctly assigned to the leg that is performing the movement.

Adaptive thresholds and FF range duration calculation. The adaptive

Table 1
Gait events and corresponding decision rules of FSM in H-GED algorithm.

Condition	Gait Events	Decision Rules
1	r_{HS}	$(accV_n.diff < 0) \& (accV_{n-1}.diff > 0) \& (accV_n.diff > th_{r_{HS}}) \& (acc_index \geq pos_{r_{HS}n-1} + range_{r_{HS}})$
2	r_{FF}	$(accV_n.diff < 0) \& (accV_{n-1}.diff > 0) \& (accV_n.diff > th_{r_{FF}}) \& (acc_index \geq pos_{r_{FF}n-1} + range_{r_{FF}})$
3	l_{TO}	$(accV_n.diff > 0) \& (accV_{n-1}.diff < 0) \& (accV_n.diff < th_{l_{TO}}) \& (acc_index \geq pos_{l_{TO}n-1} + range_{l_{TO}})$
4	r_{MSt}	$(accV_n.diff < 0) \& (accV_{n-1}.diff > 0) \& (accV_n.diff > th_{r_{MSt}}) \& (acc_index \geq pos_{r_{MSt}n-1} + range_{r_{MSt}})$
5	r_{HO}	$(accV_n.diff > 0) \& (accV_{n-1}.diff < 0) \& (accV_n.diff < th_{r_{HO}}) \& (acc_index \geq pos_{r_{HO}n-1} + range_{r_{HO}})$
6	l_{HS}	$(accV_n.diff < 0) \& (accV_{n-1}.diff > 0) \& (accV_n.diff > th_{l_{HS}}) \& (acc_index \geq pos_{l_{HS}n-1} + range_{l_{HS}})$
7	l_{FF}	$(accV_n.diff < 0) \& (accV_{n-1}.diff > 0) \& (accV_n.diff > th_{l_{FF}}) \& (acc_index \geq pos_{l_{FF}n-1} + range_{l_{FF}})$
8	r_{TO}	$(accV_n.diff > 0) \& (accV_{n-1}.diff < 0) \& (accV_n.diff < th_{r_{TO}}) \& (acc_index \geq pos_{r_{TO}n-1} + range_{r_{TO}})$
9	l_{MSt}	$(accV_n.diff < 0) \& (accV_{n-1}.diff > 0) \& (accV_n.diff > th_{l_{MSt}}) \& (acc_index \geq pos_{l_{MSt}n-1} + range_{l_{MSt}})$
10	l_{HO}	$(accV_n.diff > 0) \& (accV_{n-1}.diff < 0) \& (accV_n.diff < th_{l_{HO}}) \& (acc_index \geq pos_{l_{HO}n-1} + range_{l_{HO}})$

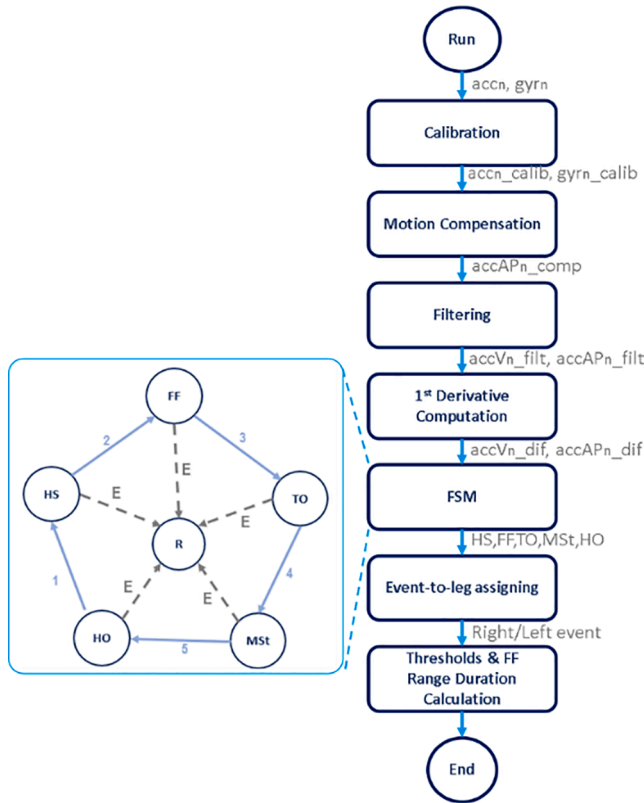


Fig. 5. Computational method for the real-time gait events detection adapted to patients with PD (PD-GED): flowchart of the proposed gait monitoring system adapted to patients with PD.

thresholds (th_{HS} , th_{FF} , th_{TO} , th_{MSt} and th_{HO}) are calculated as previously in H-GED, but the events range duration needed to be adjusted (Fig. 6. C). Instead of calculating an interval for each event, only an interval for the FF event was calculated, because it corresponds to the most prominent acceleration peak in the patients' acceleration signals. Therefore, after the occurrence of five gait cycles, each of the FF peaks were detected based on their respective peak in the previous gait cycle ($pos_{r_{FF}n-1}$). The FF peaks were considered valid only if they belong to an average of event ranges calculated every five gait cycles ($range_{r_{FF}}$).

2.4. Gait parameters estimation

Spatiotemporal gait parameters estimation is based on the detected HS gait event (initial contact) from H/PD-GED (Del Din, Hickey et al., 2016). *Step duration* and *stride duration* are estimated as follows:

$$step\ duration_i [s] = t_{i+1}HS - t_iHS \quad (1)$$

$$stride\ duration_i [s] = t_{i+2}HS - t_iHS \quad (2)$$

where, t_iHS correspond to the instants at which occurs the HS, and $t_{i+1}HS$ and $t_{i+2}HS$ are the instants that occurs the follow TOs.

To estimate *steplength* $[m]$ it is used the inverted pendulum method, which is based on the assumption of a compass gait cycle and that the vertical movement of the center of mass during a step (between the left and right HS) can be approximated to the one described by a point mass suspended at the end of an inverted pendulum, as described in (Del Din, Hickey et al., 2016). The method needs the height (L : pendulum length), experimentally measured from the floor to the place where the sensor is located, and the height of the center of mass during the step (h), which can be obtained by the double integration of the vertical acceleration (a_v). To overcome some drift in cumulative integration, we filter the vertical acceleration with zero-lag band-pass Butterworth Filter of 4th order (cut-off frequencies of 0,1 and 5 Hz) as described in (Zijlstra & Hof, 2003; Del Din, Hickey et al., 2016):

$$step\ length_i [m] = 2\sqrt{2Lh - h^2} \text{ for } h = \int_{t_{i,HS}}^{t_{i+1,HS}} a_v dt. \quad (3)$$

The stride length was estimated as the sum of two consecutive steps (e.g., right leg step plus left leg step), as described by the following equation:

$$stride\ length_i [m] = step\ length_i + step\ length_{i+1} \quad (4)$$

Gait velocity is obtained by dividing the *steplength* $_i$ by the *stepduration* $_i$:

$$gait\ velocity_i [m/s] = step\ length_i / step\ duration_i \quad (5)$$

Cadence gait temporal parameter was assessed as follows:

$$cadence [steps/min] = gait\ velocity_i \hat{\cdot} 60 / step\ length_i \quad (6)$$

3. Experimental validation

Experimental validation considered two different experiments. In Experiment I, our solution was benchmarked against a robust 3D motion analysis based on capture cameras Vicon®, with healthy subjects, running the H-GED software routines for gait events detection. In Experiment II, PD-GED software routines adapted for PD patients were used and validated against a well-studied wearable IMU-based system, Xsens®, in a hospital environment, with PD patients. The experimental protocols aimed to evaluate the efficiency of the system (i) to segment gait for different walking conditions and (ii) to estimate spatiotemporal parameters, through repeated measures of gait patterns recorded in different gait situations.

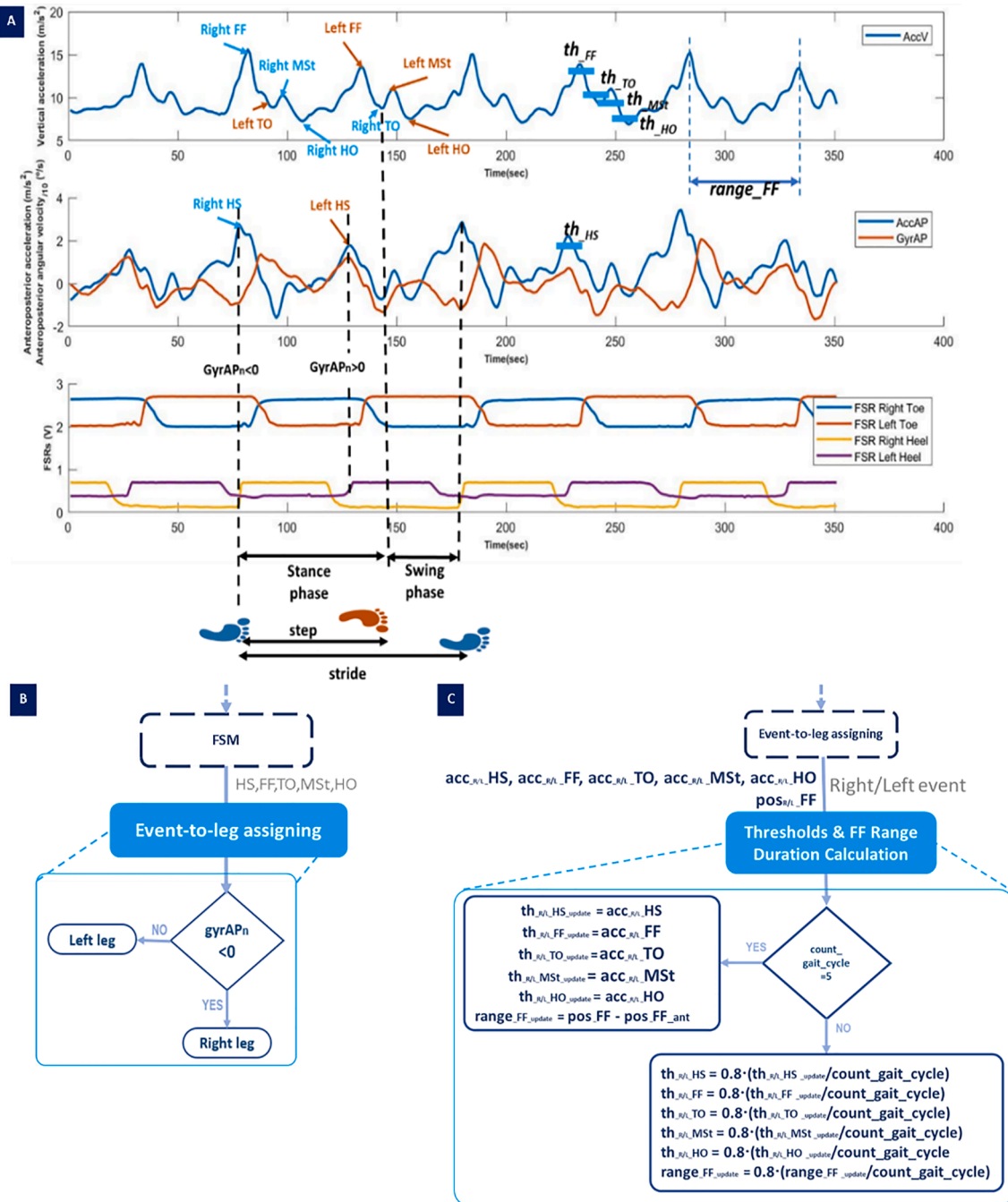


Fig. 6. A. **Top:** Lower trunk vertical acceleration for a patient with PD; **A. Middle:** Anteroposterior acceleration and angular velocity; **A. Bottom:** Force sensor resistive output for a patient with PD. Highlights for gait events over a stride, adaptive thresholds, and FF range. **B:** Zoom-in flowchart stage Event-to-leg assigning of the proposed method; **C:** Zoom-in flowchart stage Thresholds & FF Range Duration Calculation of the proposed method.

3.1. Experiment I

3.1.1. Participants

Ten healthy participants (8 males and 2 females) were involved in five walking condition trials. These participants present a 25.50 ± 2.01 years old mean \pm standard deviation age, a 71.95 ± 10.09 Kg mean \pm standard deviation weight and a mean \pm standard deviation height of 175.70 ± 8.41 cm. They signed a written informed consent to participate in this study. The study was conducted according to the rules of ethical conduct of the Life and Health Sciences defined by the University of Minho Ethics Committee CEICVS 006/2020, addressing the principles of the Declaration of Helsinki and the Oviedo Convention.

3.1.2. Experimental protocol

Fig. 7 depicts the experimental setup on the laboratory environment assessment (Fig. 7.A and .B) and the protocol timeline followed in Experiment I (Fig. 7.C). After following the VICON® protocol calibration, a START trigger was supplied from a tablet to the VICON® base station and to the instrumented waistband (TO) to start data acquisition, in order to synchronize data acquisition between both systems. Then, participants accomplished one of the five pre-defined walking trials (T1): (1) walk 10 m, turn for a preferred side, and return to the started point (vV11); (2) walk 10 m, turn to the side opposite to condition (1), and return to the starting point (vV12); (3) walk 10 m while accomplishing a trunk pitch movement, and return to the starting point (vVP); (4) walk 10 m while accomplishing a trunk roll movement, and return to

Table 2
Gait events and corresponding decision rules of FSM in PD-GED algorithm.

Condition	Gait Events	Decision Rules
1	HS	$(accAP_n.diff < 0) \ \& \ (accAP_{n-1}.diff > 0) \ \& \ (accAP_n.diff > th_{HS})$
2	FF	$(accV_n.diff < 0) \ \& \ (accV_{n-1}.diff > 0) \ \& \ (accV_n.diff > th_{R,FF}) \ \& \ (acc_index \geq pos_{R,FF_{n-1}} + range_{R,FF})$
3	TO	$(accV_n.diff > 0) \ \& \ (accV_{n-1}.diff < 0) \ \& \ (accV_n.diff < th_{TO})$
4	MSt	$(accV_n.diff < 0) \ \& \ (accV_{n-1}.diff > 0) \ \& \ (accV_n.diff > th_{MSt})$
5	HO	$(accV_n.diff > 0) \ \& \ (accV_{n-1}.diff < 0) \ \& \ (accV_n.diff < th_{HO})$

the starting point (vVR); and (5) walk 10 m and overcome a step fitness (vVS). Participants performed these five walking trials sequentially for a comfortable (“normal”) (NVw), a slow (SVw), and a fast velocity (FVw). When participants returned to the start position, a new trigger was supplied to both systems in order to stop data acquisition (T2). Vicon® motion capture system was used to establish the ground-truth. Vicon Nexus User-Interface provided the software-tools for kinematic data analysis (Vicon, 2010). VICON® system was set to acquire the 3D motion capture at 100fps to match our acquiring sample rate. It was used the Full-body Model Plug-in to place the markers on participants’ body, as depicted in Fig. 7.B. In order to eliminate any acquisition bias and consequent statistical analysis, sensors were positioned in the participants’ bodies using the same anatomical reference and by the same team member.

3.1.3. Data analysis

The acquired inertial data and reference gait events were stored as text files on a SD card, using the data storage system integrated on the waistband, for a subsequent validation through Matlab® (2018a, The Mathworks, Natick, MA, USA). We focused our data analysis in three main goals.

First, to evaluate the performance of H-GED algorithm, the detected

gait events were compared with the identified events from VICON®, considering the position of the markers on the feet, for each gait cycle, being analyzed a total of 2022 steps from both feet. From position analysis of the markers on feet, gait events were identified and compared with our identifications from H-GED. From the SD card module, we download the inertial signals and the gait events detected in real-time (expressed by saving the FSM states) during the experimental tests. These values were used to compare against the synchronized ground-truth systems. Detected gait events were evaluated considering their sensitivity (Eq. (7)) and accuracy (Eq. (8)). True positives (TP) corresponded to the gait events correctly identified, true negatives (TN) concerned to gait events that the algorithm correctly detected as a non-event, false positives (FP) regarded to gait events not correctly identified and false positives (FN) framed to events that should had been detected. Earlier and delayed detections were also evaluated based on their percentage of occurrence, duration, and impact on a gait cycle duration (range of motion error (ROME) calculation). Earlier and delayed detections were considered from the TP detections.

$$Sensitivity = TP / (TP + FN) \tag{7}$$

$$Accuracy = (TP + TN) / (TP + TN + FP + FN) \tag{8}$$

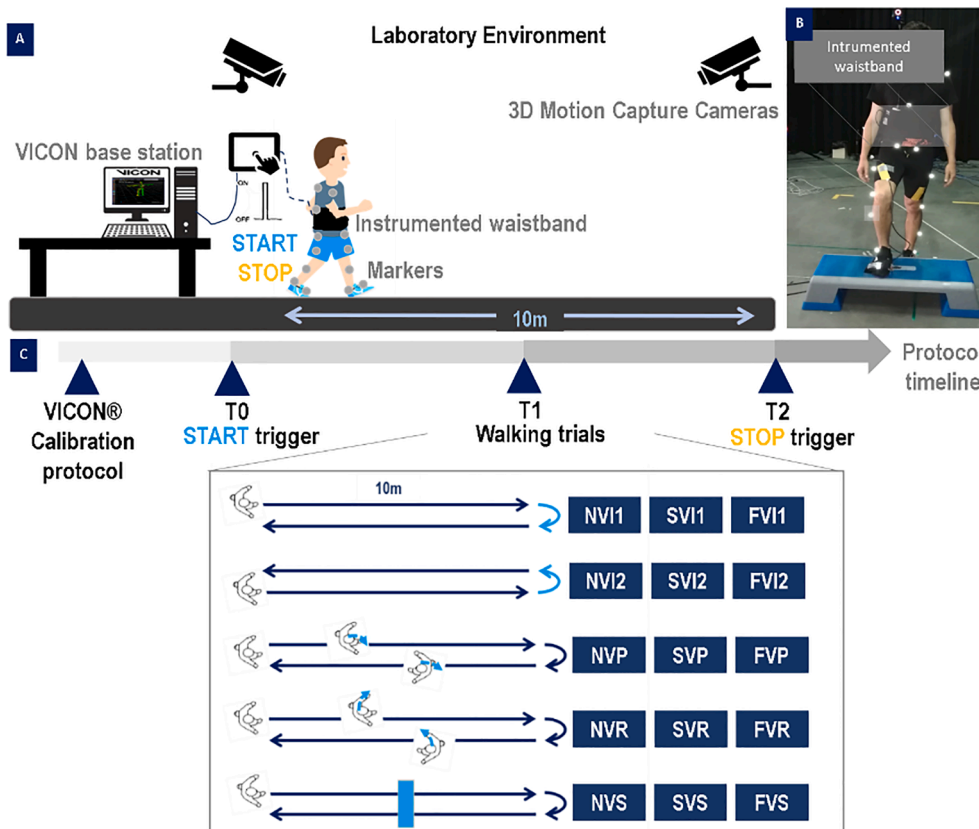


Fig. 7. A: Experimental setup of the laboratory environment assessment in Experiment I; B: Participant instrumented with the VICON® markers and the proposed instrumented waistband; C: Experimental protocol steps of Experiment I.

Second, FSM adaptability and events range duration were graphically demonstrated. Furthermore, sensitivity and accuracy metrics were also estimated to analyze the impact of applying adaptive thresholds and a motion compensation strategy in H-GED algorithm performance considering three conditions: (1) with adaptive thresholds & events range duration and with motion compensation (final solution); (2) with static thresholds and events range duration; and (3) without motion compensation. To evaluate the ability of the motion compensation routine implemented in the gait events detection, we compared the pitch and roll angles estimated by our proposed solution and the angles measured with the ground-truth system in the respective marker placed on the same body location (L5). Therefore, we analyzed the ROM per stride for each angle and after checking normality, we tested the hypothesis that there are no statistically significant differences in the angles measured with both systems ($p > 0.05$). Also, the root-mean-square deviation (RMSD) and the normalized root-mean-square deviation (NRMSD) were calculated as magnitude-based deviation measurements. Lastly, we assessed the waveform similarity from the average ROM of vertical acceleration acquired with our sensor and the respective marker placed on the same body location (L5). Also, the deviation error measurements were analyzed, namely RMSD and NRMSD.

Third, we used statistical analysis based on the percentage of absolute error ($\epsilon\%$) to address a benchmarking analysis of gait parameters estimation and often used to measure the error of new proposed solutions (Jakobsen, Gluud, Winkel, Lange, & Wetterslev, 2014). For that, we estimated the absolute difference between the corresponding gait spatiotemporal parameters with both systems, assuming the Vicon® measurements as the true reference. Further, it was used a classification criterion of acceptability to provide a reliability assessment of the percentage of absolute error that enabled to characterize the obtained results (Fusca et al., 2018). The adopted criterion is based on four categories defined by standard statistical thresholds for significance analysis (Jakobsen et al., 2014) and able to classify as: (1) Excellence: if $\epsilon\% < 5\%$; (2) Good: if $5\% \leq \epsilon\% < 10\%$; (3) Sufficient: if $10\% \leq \epsilon\% < 20\%$; and (4) Not acceptable: if $\epsilon\% \geq 20\%$.

3.2. Experiment II

3.2.1. Participants

Twenty patients with idiopathic PD participated in Experiment II (12

males and 8 females). These participants present a 67.70 ± 9.68 years old mean \pm standard deviation age, a 69.30 ± 11.60 Kg mean \pm standard deviation weight, and a 162 ± 4.75 cm mean \pm standard deviation height. Further, they were assessed based on PD scales, namely the H&Y scale, with a 2.1 ± 0.54 mean \pm standard deviation; and the UPDRS-III with a 25.80 ± 8.13 mean \pm standard deviation score. All patients gave informed consent and the study granted ethical approval by the Hospital of Braga Ethical Commission 36/2018, following the principles of the Declaration of Helsinki and the Oviedo Convention. Patients were recruited if they present $H\&Y \leq 3$, age between 50 and 85 years old, do not have cognitive impairment, present autonomous gait and are evaluated by neurologists. All patients when performed the clinical trials were in the ON phase.

3.2.2. Experimental protocol

Fig. 8 depicts the experimental setup on the clinical environment assessment (Fig. 8.A and .B) and the protocol timeline followed in Experiment I (Fig. 8.C). Experimental protocol steps included a first phase of Xsens® calibration. To start data acquisition, a trigger was sent from instrumented waistband to Xsens® base station (T0). Subsequently, participants performed one of the required walking trials (T1) for a distance of 10 m on unobstructed hallway, at three different gait velocities (NV - normal velocity, SV - slow velocity and FV - fast velocity). Each participant performed 3 trials for each gait velocity, performing a total of 9 walking trials. At the end of the walking trial, a stop trigger was supplied from the instrumented waistband to the Xsens® base station (T2). Data acquisition was started/stopped via Bluetooth by a mobile APP. Between velocity change trials, the waistband was removed and then replaced to assess test–retest repeatability. The MVN BIOMECH system from Xsens®, an ambulatory 3D human kinematic measurement system, was employed as ground-truth. We centered the analysis in the kinematic data for gait analysis and it was used the Lower Body Plug-in to place the inertial sensors, being used seven sensors, as depicted in Fig. 8.C (the same team member always placed the sensors on the participant). The ground-truth system recorded the inertial information at 100 Hz to guarantee the synchronism between both systems. This is a well-established IMU-based system for benchmarking analysis, able to track the human gait indoors and outdoors (Technologies, 2018).

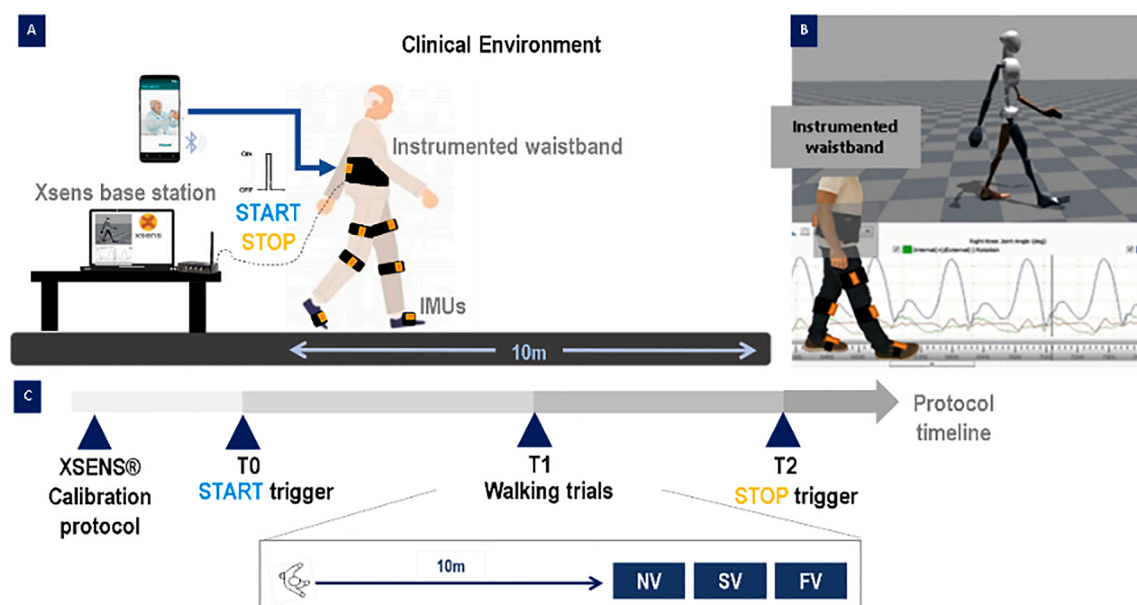


Fig. 8. A: Experimental setup of the clinical environment assessment in Experiment II; B: Participant instrumented with the Xsens® inertial units and the proposed instrumented waistband; C: Experimental protocol timeline of Experiment II.

3.2.3. Data analysis

A total of 4236 steps from both feet were analyzed through Matlab®. For each gait cycle, the real-time detected gait events (stored on the SD card module) were compared with the output events from Xsens® regarding its sensitivity (Equation (7)), accuracy (Equation (8)) and earlier and delayed detections by its percentage of occurrence, duration, and ROME (as described in Experiment I). The adaptability and FF range duration of the FSM were graphically presented. To address a benchmarking analysis of gait parameters estimation, we computed the percentage of absolute error ($\epsilon\%$), assuming the Xsens® outcomes as the reference data. A reliability assessment on the obtained percentages of absolute error was conducted by means of the standard statistical thresholds 5%, 10%, and 20%, which enabled to classify the error acceptability as excellence (for $\epsilon\% < 5\%$), good (if $5\% \leq \epsilon\% < 10\%$), sufficient (if $10\% \leq \epsilon\% < 20\%$), and not acceptable (in case of $\epsilon\% \geq 20\%$).

Lastly, it was accomplished a study between the measured gait parameters for the trials with normal velocity (NV) and the patients' stage in UPDRS-III and H&Y scales. UPDRS-III scale patients in terms of their motor function, while the H&Y assesses how symptoms evolve with disease progression. We investigated whether the measured gait spatiotemporal parameters corresponded to motor impairments and illness stage defined by the UPDRS-III and H&Y scales. The UPDRS-III scale is associated with lower extremity function, so based on (Schlachetzki et al., 2017), we grouped the patients according to the level of their motor impairment scores in three groups: UPDRS-III low (L):1–12 (N = 2); UPDRS-III middle (M):13–23 (N = 4); and UPDRS-III high (H) ≥ 23 (N = 14). Regarding H&Y scale, based on (Perlmutter, 2009), patients were grouped by their stage: 1 – unilateral disease (N = 2); 2 – bilateral disease (N = 14); and 3 – mild to moderate bilateral disease (N = 4). Table 3 summarizes this information. Then, the measured group stride duration, stride length, step duration, step length, velocity and cadence were analyzed (cross-sectional study) according to the UPDRS-III and H&Y stage. Data were observed through the mean of the estimated gait parameters and standard error measurement (SEM). SEM is the quotient between the standard deviation for the square root of the sample size, which allows comparing the dispersion of values between groups.

4. Results

4.1. Results of experiment I

1) *Performance metrics for H-GED algorithm.* Table 4 presents the performance of the real-time algorithm for gait events detection (H-GED) against the ground-truth outcomes (Vicon® system), for the different walking conditions (vVw). It shows the H-GED sensitivity, accuracy and, earlier and delayed detections (by means of their percentage of occurrence, duration, and ROME).

2) *FSM adaptability & motion compensation analysis.* We highlight in Fig. 9.A how the proposed adaptative thresholds and events range duration progress over walking time for a participant in first trial (NV1). It is depicted the adaptive thresholds associated to the amplitude of the acceleration signal ($th_{R/L,HS}$, $th_{L,R/L,FF}$, $th_{R/L,TO}$, $th_{R/L,MSt}$ and $th_{R/L,HO}$) and the events range duration ($range_{R/L,HS}$, $range_{R/L,FF}$, $range_{R/L,TO}$, $range_{R/L,MSt}$ and $range_{R/L,HO}$). Note that the proposed thresholds, used in the decision rules, were adaptively calculated every

five gait cycles and the first thresholds were set empirically. Also, it is possible to observe that the events range duration, after five strides, were adaptively calculated every three gait cycles. In addition, we verified that the algorithm's adaptability provides a proper detection of the ten proposed gait events: 1 – Right HS, 2 – Right FF, 3 – Left TO, 4 – Right MSt, 5 – Right HO, 6 – Left HS, 7 – Left FF, 8 – Right TO, 9 – Left MSt, and 10 – Left HO.

An increase in gait speed results in higher values of lower trunk acceleration with shorter gait cycles, supporting the need to update the thresholds and events range duration (Auvinet et al., 2002). Therefore, as a title of example, it is depicted in Fig. 9.B the thresholds associated to a maximum and minimum peak in acceleration signal ($th_{R,HS}$ and $th_{R,TO}$, respectively) and an event range ($range_{R,HS}$) behavior, for the same participant's walking task (v11) for normal, slow and fast velocity. We observed that for slow velocities, the thresholds' values decrease for lower magnitude of the maximums and minimums. Likewise, for lower velocities, there is an increase in gait cycles duration, so the event ranges are higher. Conversely, when the velocity is faster, the values of the thresholds increase and the events range duration decrease.

Table 5. presents the outcomes from the analysis on H-GED sensitivity and accuracy when applying (i) adaptive thresholds & events range duration and motion compensation (Condition (1)), (ii) static threshold (Condition (2)) and (iii) without motion compensation (Condition (3)). It was observed that H-GED algorithm performance decreases when it is used static thresholds and events range duration (Condition (2)) and without motion compensation (Condition (3)). We concluded that the inclusion of a versatile algorithm and application of a motion compensation strategy results in a higher performance.

We compared the estimated pitch and roll angles estimated by our proposed solution and the ground-truth system. Table 6 presents the ROM per stride, RMSD and NRMSD computed from the values of angles estimation for the different trials (vVw). There were not statistically differences between the estimated angles with both systems ($\rho \geq 0,10$). Also, the error deviation measurements, RMSD and NRMSD, exhibit low mean values (Pitch estimation: RMSD = 6,42° and NRMSD = 6,90%; Roll estimation: RMSD = 6,68° and NRMSD = 6,44%). The worst error deviation measurements were obtained for the trials with higher velocities (FVw) and for the trials which included the walking task for perform the pitch/roll trunk movement (vVP and vVR). Table 6 also shows the ROM per stride, RMSD and NRMSD computed from the average values of vertical acceleration for the different trials (vVw). There is a similarity between the signals ($\rho \geq 0,19$) for the different walking trials, highlighting the low deviations between the signals acquired (total mean of 3.11 m²/s for RMSD and 4,91% for NRMSD). The trials which involved a fast velocity (FVw), obtained the highest values of deviation (RMSD $\geq 2,77$ m/s²; NRMSD $\geq 4,50\%$, $\rho \geq 0,19$), as well as the walking conditions which included the use of a step (vVS) (RMSD $\geq 2,73$ m/s²; NRMSD $\geq 4,57\%$, $\rho \geq 0,19$). Probably because the sensor is more susceptible to movement artifacts for faster walking and when it was required to overcome a step.

3) *Benchmarking analysis of gait parameters estimation.* To accomplish a benchmarking analysis of gait parameters estimation it is highlighted in Table 7 the percentage of absolute error ($\epsilon\%$) measured between the estimated values (stride duration, stride length, step duration, step length, velocity and cadence) with our system and the ground-truth system (reference system), for the different trials (vVw). Also, it shows the mean percentage of absolute error assuming the variable velocity for trials (last column). We used a reliability standard statistical threshold for significance analysis to classify the error estimation as excellent, good, sufficient, and not acceptable, represented by colors in Table 7.

The highest percentage of absolute error was obtained when calculating the step length for a slow velocity ($\epsilon\%=12,94\%$). The worst percentages of absolute error were obtained for trials which involved a slower speed (SVw: $\bar{x} \pm SD = 0,80 \pm 0,03$ m/s). The gait parameters estimation depends on the detection of gait events, namely HS, a fact that could explain the higher error values obtained in these trials, since

Table 3
Patients grouped regarding UPDRS-III an H&Y scales.

UPDRS - III	Low (Score: 1–12)	N = 2
	Medium (Score: 13–23)	N = 4
	High (Score ≥ 23)	N = 14
H&Y	Unilateral disease (Score: 1)	N = 2
	Bilateral disease (Score: 2)	N = 14
	Mild to moderate bilateral disease (Score:3)	N = 4

Table 4

H-GED algorithm performance for gait events detection for the different trials (vVw), regarding sensitivity (Sens.), accuracy (Acc.), earlier and delayed detections (percentage of occurrence (%), duration ($\bar{x} \pm SD$ ms), ROME(%), mean \pm standard deviation ($\bar{x} \pm SD$) for the velocity measured with the ground-truth system and total participants' number of steps for each trial.

Trial	Sens. [%]	Acc. [%]	Earlier (E)			Delayed (D)			Trial Velocity ($\bar{x} \pm SD$) [m/s]	Number of steps
			%	($\bar{x} \pm SD$) [ms]	ROME [%]	%	($\bar{x} \pm SD$) [ms]	ROME [%]		
NV11	97,92	94,79	17,56	12,36 \pm 4,26	0,81	12,13	11,89 \pm 2,03	0,78	0,97 \pm 0,09	139
NV12	96,56	97,48	16,13	11,73 \pm 3,29	0,82	13,86	9,99 \pm 1,26	0,70		142
NVP	98,11	93,34	10,38	12,74 \pm 3,56	0,87	14,07	10,02 \pm 3,01	0,68		136
NVR	98,90	94,93	10,26	11,41 \pm 2,98	0,80	13,84	11,34 \pm 1,21	0,79		141
NVS	97,55	91,22	13,64	12,36 \pm 4,36	0,90	14,42	12,56 \pm 0,95	0,92		128
SV11	91,91	93,24	22,96	18,44 \pm 2,56	1,04	19,33	18,74 \pm 1,01	1,05	0,80 \pm 0,03	148
SVI2	91,58	96,70	14,96	18,31 \pm 3,08	1,02	18,91	17,05 \pm 2,88	0,95		151
SVP	91,02	91,78	21,28	17,66 \pm 1,36	1,01	18,25	16,05 \pm 3,01	0,92		154
SVR	91,90	92,27	21,86	17,89 \pm 2,03	1,02	18,83	17,55 \pm 2,14	1,00		155
SVS	89,20	91,71	23,08	19,99 \pm 3,36	1,40	20,05	18,69 \pm 2,23	1,31		149
FV11	97,18	91,35	18,88	9,99 \pm 3,03	0,90	14,13	11,89 \pm 2,03	1,07	1,14 \pm 0,07	116
FVI2	97,22	95,13	20,60	9,89 \pm 3,26	0,95	13,86	9,99 \pm 1,26	0,96		116
FVP	95,44	95,41	19,33	11,35 \pm 4,01	1,12	13,07	10,02 \pm 3,01	0,99		120
FVR	96,52	94,81	18,05	10,26 \pm 2,46	1,01	14,42	9,34 \pm 1,21	0,92		116
FVS	95,34	90,51	20,88	11,33 \pm 2,46	1,10	14,84	8,56 \pm 0,95	0,83		111
Total mean	95,09	93,64	17,99	13,71 \pm 3,06	0,81	15,60	12,91 \pm 1,88	0,92	-	-

for slower velocities the gait event detection algorithm (H-GED) performance decreased. Slower velocities produce waveforms with slightly different shapes that no longer respect the designed rules. We can infer that the efficiency of detecting gait events influences the estimation of gait parameters. Even so, the errors obtained were mostly categorized as good ($5,15\% \leq \epsilon\% \leq 15,98\%$, highlighted as blue) and, for the trials with velocity closest to the participants' comfortable speed (NV), we obtained excellent error classification ($3,02\% \leq \epsilon\% \leq 4,59\%$, highlighted as green).

4.2. Results of Experiment II

1) *Performance Metrics for PD-GED algorithm.* Table 8 shows the performance of the algorithm for gait events detection adapted for patients with PD (PD-GED) against the ground-truth data (Xsens® system). For the different trials (vV), we investigated the sensitivity, accuracy and earlier and delayed detections (regarding their percentage of occurrence and ROME).

The proposed method showed to be significantly sensitive (total mean of 99,53%) and accurate (total mean of 97,42%) for detection of all events at distinct velocities. When participants accomplished the walking trials with a slower velocity (SV: $0,71 \pm 0,06$ m/s), the results showed the worst performance for gait events detection (sensitivity = 99,42% and accuracy = 96,49%). As previously obtained, this may be due to the lower prominence of the acceleration peaks observed in slower velocities, making difficult the detection of maximums/minimums. From the earlier and delayed detection analysis, it is highlighted the time-effectiveness of the proposed computational method, given their low mean percentages (E: 16,73% and D: 16,25%). There are not high differences between the earlier and delayed detections (E: $2,94 \pm 4,32$ ms and ROME = 0,82%; D: $12,71 \pm 1,31$ ms and ROME = 0,91%). The worst values were obtained for trials with lower velocities but did not contribute with significant early/delays in gait detection, since their impact on a gait cycle was very low (ROME $\leq 0,91\%$). As anticipated, the total number of steps increases for slower velocities.

2) *FSM adaptability.* Fig. 10.A shows the adaptive thresholds associated to the amplitude of the acceleration signal HS/TO/MSt threshold (th_{HS} , th_{FF} , th_{TO} , th_{MSt} and th_{HO}) and FF range ($range_{FF}$) for a subject with normal walking velocity. Firstly, we observed that the adaptive thresholds and FF range duration were adaptively computed every five gait cycles and the first thresholds were set empirically. This confirms the detection of all proposed gait events: 1 - HS, 2 - FF, 3 - TO, 4 - MSt, and 5 - HO. Note that due to the adaptation performed in the FSM oriented to patients with PD, a complete gait cycle involves two cycles of FSM states, being each event assigned to the leg which performed the

gait event. Fig. 10.B also depicts the progress of the adaptive thresholds (th_{HS} and th_{TO} , as example) and FF range for a participant walking at normal, slow and fast velocity. As expected, we verified that the values of the thresholds increase or decrease when the gait velocities are slower or faster, respectively. Also, the FF range duration is equally affected by the duration of the gait cycles. Gait speed affects the magnitude of maximums and minimums of acceleration signal and gait cycles duration, being needed the adaptation of thresholds and FF range. Lastly, we observed that in the trial with fast gait velocity, as it was expected, the participant travelled the trial distance in less time, with shorter gait cycle times and with a greater number of steps (highest occurrence of gait cycles - 2 loops in FSM).

3) *H-GED & PD-GED performance vs H&Y scale.* We asked what would be the performance of the gait events detection algorithm according to the degree of the disease (H&Y scale), comparing the measured performance metrics of PD-GED and H-GED. We grouped the measured performance metrics according H&Y stages, as depicted in Fig. 11. For healthy subjects, H&Y is scored as null, and as the disease progress H&Y is scored by 1,2 and 3. We observed that as the disease evolves, the performance of the algorithm decreases and the trials with patients showed a better performance, since included simple walking trials. We also observed that all groups showed a decrease in performance for lower trial velocities.

4) *Benchmarking analysis of gait parameters estimation.* The percentage of absolute error ($\epsilon\%$) measured for the different trials (vV_x) between the estimated values of gait parameters (step/stride duration/length, velocity and cadence) with our system and the ground-truth system (reference system), is presented in Table 9.

The worst result was measured for the estimation of the step length for a slow velocity (SV_x: $\epsilon\% \leq 13,45\%$). We believe that the step length estimation presents the worst results, as opposed to the temporal parameters, since it depends on more variables than HS detection (Equation (3)). This parameter depends on the height from the floor to the place where the sensor is located, and the height of the center of mass during step, so this calculation may introduce some error that can justify the measured errors. However, from the analysis of the statistical thresholds of the standard of reliability (Table 9), we found that the mean percentages of absolute error are often classified as good (highlighted at blue: $5,48\% \leq \epsilon\% \leq 9,14\%$) and excellent (highlighted at green: $2,81\% \leq \epsilon\% \leq 4,88\%$).

5) *Gait parameters estimation vs clinician scales.* Fig. 12 depicts the estimated gait parameters (step/stride duration/length, velocity, and cadence) in accordance with UPDRS-III and H&Y stage groups, displayed as mean \pm SEM. It is highlighted that the patients assessed as

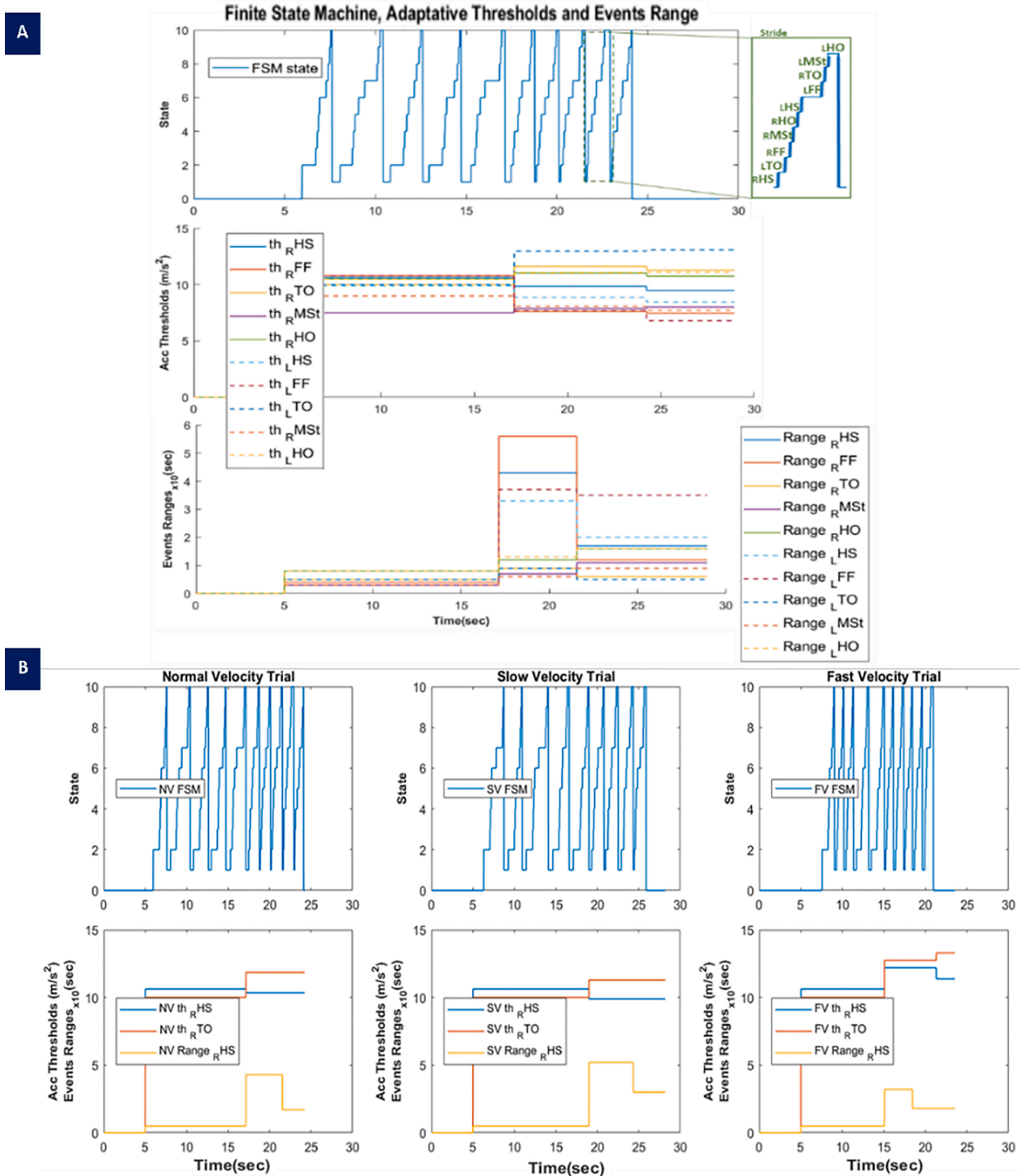


Fig. 9. A: Representation of the adaptive thresholds ($th_{R/L,HS}$, $th_{R/L,FF}$, $th_{R/L,TO}$, $th_{R/L,MSt}$ and $th_{R/L,HO}$) and events range duration ($range_{R/L,HS}$, $range_{R/L,FF}$, $range_{R/L,TO}$, $range_{R/L,MSt}$ and $range_{R/L,HO}$) over the time, for a subject in first trial (VN1) considering the different detected states of the FSM (H-GED). B: Representation of the adaptive thresholds ($th_{R,HS}$ and $th_{R/L,TO}$) and events range duration ($range_{R,HS}$) for the same subject's walking task (v1) for normal (NV), slow (SV) and fast (FV) velocity, highlighting the FSM states.

having a higher motor level impairment (UPDRS-III high ≥ 23 , $N = 14$) presented the prototypical *parkinsonian* gait parameters: decreased spatial parameters, while increased temporal parameters (Schlachetzki et al., 2017). Indeed, according to sub-item 25 of the UPDRS-III, which evaluates *parkinsonian* gait, clinicians evaluate gait observing mainly changes in gait velocity and step length (Perlmutter, 2009). Thus, we verified if the same tendency was verified with the gait parameters measured by the proposed system. We observed that averaged gait

velocity and step length decreased with disease severity, corresponding to the clinician's rating of the sub-item 25 of UPDRS-III. Further, it was observed an increase in temporal parameters for patients with high UPDRS-III. When grouping the patients according to the disease stage of H&Y scale, the same pattern was observed. Patients in a more advanced disease stage (H&Y rated of 3) presented a lower averaged velocity, shorter steps/strides length, and higher temporal parameters (step/stride duration and cadence). These outcomes agree with what is

Table 5

H-GED algorithm performance for gait events detection for the different trials (vVw), regarding sensitivity (Sens.), accuracy (Acc.), for the different walking trials (vVw), considering three conditions: (1) with adaptive thresholds & events range duration and with motion compensation (final solution); (2) with static thresholds and events range duration; and (3) without motion compensation.

Trial	Condition (1)		Condition (2)		Condition (3)	
	Sens. [%]	Acc. [%]	Sens. [%]	Acc. [%]	Sens. [%]	Acc. [%]
NVI1	97,92	94,79	92,90	91,29	94,30	93,34
NVI2	96,56	97,48	88,39	89,78	93,08	91,45
NVP	98,11	93,34	89,09	86,04	92,73	91,00
NVR	98,90	94,93	89,37	86,32	92,38	91,97
NVS	97,55	91,22	92,00	82,50	94,89	86,16
SVI1	91,91	93,24	82,70	82,82	86,70	89,07
SVI2	91,58	96,70	79,90	82,14	82,87	86,81
SVP	91,02	91,78	81,14	78,90	85,68	85,15
SVR	91,90	92,27	80,31	79,34	84,86	85,22
SVS	89,20	91,71	78,85	78,98	83,01	85,09
FVI1	97,18	91,35	90,11	86,11	93,11	90,28
FVI2	97,22	95,13	93,31	91,11	95,13	92,78
FVP	95,44	95,41	92,47	91,00	94,29	92,73
FVR	96,52	94,81	92,67	90,10	94,67	91,99
FVS	95,34	90,51	92,50	86,70	95,00	88,70
Total mean	95,09	93,64	87,71	85,54	90,85	89,45

expected and assessed by clinicians. Analyzing SEM behavior, it was observed low dispersed values between each group, which could determine a typical pattern of disease level.

5. Discussion

5.1. Experiment I

A real-time gait monitoring system was validated using repeated measures of healthy gait patterns. We analyzed its performance for gait events detection (H-GED algorithm) and benchmarked for gait parameters estimation. Also, we analyzed the contribution of the application of an adaptive and dynamic FSM behavior instead of the traditional static pattern. Motion compensation strategy contribute was also assessed by measuring the algorithm performance with and without motion compensation and by an analysis on lower trunk pitch and roll angles estimations. Our solution was validated against a camera-based motion capture system and participants performed functional tasks resembling

near-daily walking tasks (different walking velocities, reversing gait, trunk movements and passing through obstacles), opposed to what is generally addressed in (Morris et al., 2019), (Zago et al., 2018) and (Fusca et al., 2018), as they only considered free walking.

The proposed algorithm showed to be significantly sensitive (total mean of 95,09%) and accurate (total mean of 93,64%) for most of the tested gait tasks. As measured in (González, López, Rodríguez-Uría, Álvarez, & Alvarez, 2010; McCamley et al., 2012; Zijlstra & Hof, 2003), we also observed that lower gait speed decreases the accuracy of gait event estimation, perhaps because it is a less natural and fluid gait for the participants, and the resulting acceleration waveforms no longer respect the normal shapes, affecting the moments of detection of the expected gait events given the low magnitude of the acceleration signal. Nonetheless, we believe that these outcomes did not have a high impact in real-time application, given the obtained accuracy and sensitivity values are still significant good.

An efficient temporal performance was also another feature observed in our computational method. The algorithm proved to be time-effective for the different trials, showing earlier/delays significantly close to zero (E: $13,71 \pm 3,06$ ms; D: $12,91 \pm 1,88$ ms) and with low impact on the gait cycle (E: 0,81%; D: 0,92%). In (González et al., 2010; McCamley et al., 2012; Zijlstra & Hof, 2003) it was also presented computational methods to identify IC and FC events with good temporal performance, where González et al., 2010 had the lowest mean absolute error at 9–15 ms for initial FC detection. However, these studies did not perform a real-time detection and their validations lack validation against well-known, commercially and accepted ground-truth systems. Indeed, we obtained the lowest delayed detection of 8.56 ms measured with a pre-validated ground-truth system. Also, our system was able to advantageously conduct a more holistic gait segmentation by detecting five gait events for each leg, more than what is discussed in (Alvarez et al., 2010; González et al., 2010; Iijima & Takahashi, 2020; McCamley et al., 2012; Trojaniello et al., 2014).

Real-time effectiveness was one of the most crucial requirements for our technology, since we consider integrating this computational method into a high-aid device for active assistance in PD. When comparing our outcomes with the literature regarding real-time implementation based on a FSM for lower trunk signals analysis, we report higher temporal efficiency (D = $12,91 \pm 1,88$ ms), given that in (Alvarez et al., 2010) it was reported higher values of mean delayed detections D = $76,06 \pm 56$ ms, for real-time initial-contact and final-contact detection. However, it is important to mention that higher earlier/delayed detections were obtained in this study (E/D = $13,71 \pm 3,06$ ms/ $12,91 \pm$

Table 6

Evaluation of the Motion Compensation per stride and Signal Similarity Analysis, from proposed system (PS) and Vicon®, for the different walking trials (vVw).

Trial	Evaluation of the Motion compensation Routine								Signal Similarity Analysis							
	Pitch Estimation				Roll Estimation				ROM [m/s ²]				ρ*			
	ROM [°]		ρ*	RMSD [°]	NRMSD [%]	ROM [°]		ρ*	RMSD [°]	NRMSD [%]	ROM [m/s ²]		ρ*	RMSD [m/s ²]	NRMSD [%]	
	PS	V				PS	V				PS	V				
NVI1	5,39	5,49	0,18	8,58	9,75	6,22	7,24	0,45	6,75	8,17	9,29	9,01	0,75	2,27	3,90	
NVI2	3,92	2,96	0,17	9,24	8,10	4,85	5,79	0,55	8,58	10,91	9,12	9,76	0,44	2,47	4,08	
NVP	4,08	4,34	0,16	8,48	6,25	9,64	9,59	0,30	4,70	2,07	8,14	9,46	0,45	2,76	4,26	
NVR	4,53	4,09	0,20	2,71	4,18	6,49	7,45	0,44	10,72	10,09	8,95	9,67	0,42	2,59	4,06	
NVS	8,87	7,50	0,34	8,66	12,53	6,48	6,82	0,01	9,64	8,38	14,47	13,03	0,39	4,05	6,62	
SVI1	4,37	4,37	0,25	1,37	3,07	6,17	6,09	0,03	3,10	4,31	5,63	4,98	0,19	2,57	3,95	
SVI2	3,33	3,71	0,21	2,62	1,39	6,25	6,73	0,23	4,35	3,19	6,77	5,07	0,42	2,77	4,35	
SVP	3,87	3,67	0,17	6,26	4,54	7,96	7,75	0,56	2,12	2,27	5,31	5,35	0,42	2,89	4,31	
SVR	4,12	4,96	0,19	4,08	6,75	8,71	8,59	0,44	8,64	9,54	6,21	5,41	0,43	2,05	3,22	
SVS	9,53	9,37	0,32	7,66	10,06	6,88	5,13	0,12	10,97	6,60	11,51	10,59	0,42	2,73	4,57	
FVI1	4,98	4,98	0,20	8,84	4,94	6,98	6,65	0,07	5,53	6,97	11,29	10,48	0,20	3,76	5,91	
FVI2	4,98	3,81	0,19	9,87	8,30	8,12	7,99	0,92	8,54	7,56	12,38	10,72	0,40	3,65	5,75	
FVP	4,98	3,56	0,10	5,84	6,64	8,14	10,88	0,89	6,87	4,42	10,03	10,16	0,40	2,77	4,50	
FVR	5,27	5,37	0,13	6,23	9,95	12,44	12,74	0,55	2,95	3,99	11,39	10,41	0,40	3,92	5,98	
FVS	8,20	8,07	0,19	5,89	6,99	6,22	18,24	0,05	6,75	8,17	20,20	20,23	0,19	5,52	8,19	

*Level of significance of 5%. PS – Proposed system; V – Vicon® system.

Table 7

Benchmarking analysis of gait parameters estimation. Percentage of absolute error ($\epsilon\%$) measured from the obtained gait parameters for the different walking trials (vVw) and as a mean ($\bar{x}\epsilon\%$) for each trial (NVw, SWw and FVw), and trial velocity mean \pm standard. Reliability assessment by colors: green – excellent ($\epsilon\% < 5\%$); blue – good ($5\% \leq \epsilon\% < 10\%$); yellow – sufficient ($10\% \leq \epsilon\% < 20\%$); red – not acceptable ($\epsilon\% \geq 20\%$).

Trial	Step Duration $\epsilon\%$	Stride Duration $\epsilon\%$	Step Length $\epsilon\%$	Stride Length $\epsilon\%$	Velocity $\epsilon\%$	Cadence $\epsilon\%$	Trial Velocity [m/s] ($\bar{x} \pm SD$)
NVI1	1,93	1,97	2,87	7,64	0,96	1,97	0,97±0,09
NVI1	1,93	1,97	2,87	7,64	2,61	1,97	
NVP	1,33	3,55	3,90	3,44	5,30	1,35	
NVR	13,17	1,56	5,15	2,31	15,53	15,67	
NVS	2,54	7,75	1,70	1,05	0,86	2,61	
$\bar{x}\epsilon\%$	4,59	3,44	3,02	4,20	5,05	5,15	
SVI1	7,38	4,11	15,47	5,08	7,53	6,87	0,80±0,03
SVI2	3,04	3,10	12,15	4,24	15,66	3,13	
SVP	14,31	2,81	8,48	9,23	5,10	12,52	
SVR	7,30	3,17	12,63	7,56	4,96	6,81	
SVS	8,22	6,69	15,98	10,69	7,17	7,60	
$\bar{x}\epsilon\%$	8,05	3,98	12,94	7,36	8,09	7,38	
FVI1	3,10	3,62	3,25	1,82	1,15	3,01	1,14±0,07
FVI2	8,38	1,93	2,49	3,62	5,44	7,73	
FVP	7,33	3,37	3,83	4,34	12,04	7,91	
FVR	6,29	2,07	0,82	4,87	5,84	6,71	
FVS	5,33	7,09	5,31	5,30	11,24	5,63	
$\bar{x}\epsilon\%$	6,09	3,62	3,14	3,99	6,94	6,20	

Table 8

PD-GED algorithm performance for gait events detection for the different trials (vV), regarding sensitivity (Sens.), accuracy (Acc.), earlier and delayed detections (percentage of occurrence (%), duration ($\bar{x} \pm SD$ ms) and ROME (%), mean \pm standard deviation ($\bar{x} \pm SD$) for trial velocity measured with the ground-truth system and total participants' Number of steps for each trial.

Trial	Sens.	Acc.	Earlier (E)			Delayed (D)			Trial Velocity [m/s] ($\bar{x} \pm SD$)	Number of Steps
			%	($\bar{x} \pm SD$) ms	ROME (%)	%	($\bar{x} \pm SD$) ms	ROME (%)		
NV	99,53	97,16	17,07	12,36±2,26	0,82	15,45	12,33±3,43	0,91	0,89±0,02	708
SV	99,42	96,49	14,95	15,73±3,29	0,75	18,17	14,26±2,36	1,00	0,71±0,06	858
FV	99,64	98,60	18,17	10,74±3,56	0,90	15,13	11,54±2,76	0,83	0,93±0,01	648
Total mean	99,53	97,42	16,73	12,94±4,32	0,82	16,25	12,71±1,31	0,91	-	-

1,88 ms) when compared to the values of our previous study (Gonçalves et al., 2018): E/D = 12.2 \pm 3.29 ms/9.69 \pm 7.88 ms. In our previous study (Gonçalves et al., 2018), the validation was performed under more controlled walking conditions, which did not include different tasks. Moreover, the system was validated against a less robust ground-truth system (a system based on Force Sensitive Resistors). In addition, we want the proposed solution to be able to perform real-time gait analysis, so we adopted strategies to reduce latency: (i) the use of a wired connection in the wearable sensory system; (ii) decision rules based on the processing of only one axis of kinematic data; and (iii) application of a 1st order low-pass filter that is computationally light.

To overcome the typical static behavior of FSM and offer intra-/inter-user adaptability in gait events detection, the proposed method innovatively applies adaptive thresholds and events range duration, which were adaptively calculated based on user walking. When using adaptive thresholds and events range duration instead of static thresholds, the total mean sensitivity and accuracy of the FSM improved from 87,71% and 85,54 to 95,09% and 93,64%, respectively. We observed that this feature was decisive for the gait events detection to be efficient regardless of the user and the gait tasks performed. Additionally, to the best knowledge of the authors, the state-of-the-art of gait events detection algorithms did not address this adaptability issue using static sliding windows or non-dynamic thresholds for peak detection methods (Alvarez et al., 2010; González et al., 2010; Iijima & Takahashi, 2020;

McCamley et al., 2012).

Another major advantage of the algorithm is the application of a motion compensation strategy. Sensor to world-frame transformation is often used in aviation, industry, or different inertial-based applications (Ferdinando, Khoswanto, & Purwanto, 2012; Windau and Itti, 2013, 2016). Our gait events detection endows a motion compensation strategy imported from this traditional sensor world-frame methods (Windau & Itti, 2016). Regardless of the users' trunk movement, their motion is compensated, and decision rules can be commonly applied. The application of a motion compensation strategy was essential to guarantee the detection of all gait events during different walking tasks. FSM performance increased 4.24% in sensitivity and 4.19% in accuracy when it is used the compensatory method. It was observed low error deviations in pitch (RMSD = 6,42° and NRMSD = 6,90%) and roll (RMSD = 6,68° and NRMSD = 6,44%) estimations for different walking velocities and walking tasks. In addition, no significant differences ($p \geq 0,19$) were found between the trunk acceleration signals between the systems. We believe that this system capability can offer motion compensation to the acquired inertial signals, allowing the adoption of common decision rules independently of the users' movement. Further, this aspect was innovatively introduced in the current state of the field on waist-mounted sensor algorithms for gait event detection. Although the experimental protocol included different walking tasks (trunk movements, gait inversion, overcome a step, different velocities), more

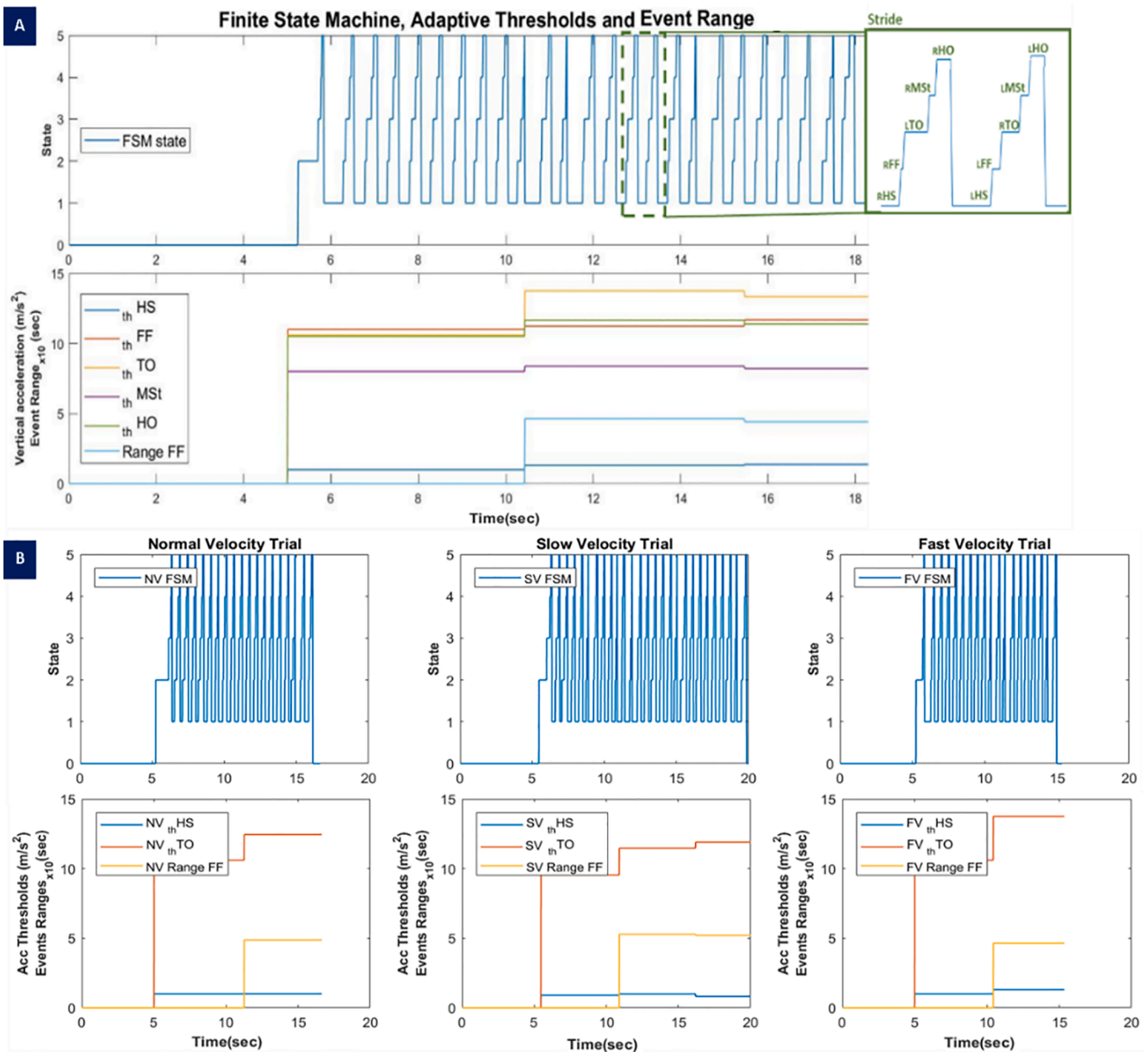


Fig. 10. A: Representation of the adaptive thresholds (th_{HS} , th_{FF} , th_{TO} , th_{MSt} , th_{HO}) and FF range over time, for a subject’s walking normal velocity trial, considering the different detected states of the FSM (PD-GED). Highlight for a gait cycle, considering two loops of FSM states, one for right and other for left leg. **B:** Representation of the adaptative thresholds (th_{HS} and th_{TO}) and FF range duration of a participant for normal (NV), slow (SV) and fast (FV) velocity trials, highlighting the FSM states.

experimental tests should be carried out to reinforce these findings, by the inclusion of walking paths with turnings, climbing stairs and use of different slopes.

Our gait analysis system besides to contribute with a gait events detector, implements a spatiotemporal gait parameters estimation. Gait events detection, particularly HS detections (foot contact), allowed the estimation of spatiotemporal parameters and a benchmarking analysis between the parameters measured with our system and ground-truth system. Our technology showed a good acceptable percentage of absolute error ($5,15\% \leq \epsilon \leq 15,98$) and, for the trials in which the participants performed at a normal (comfortable) velocity, the error classification was considered excellent ($3,02\% \leq \epsilon \leq 4,59\%$). It should be noted that the temporal parameters (step/stride duration) have less percentage of absolute error, while the spatial parameters (step/stride length, velocity) have a higher error, in particular the step length ($\epsilon \leq 12,94\%$), as is also observed in the literature (Alvarez et al., 2010; Iijima

& Takahashi, 2020; Zijlstra & Hof, 2003). Spatial parameters are derived from the step length calculation which entails some drift error on its calculation, while the temporal parameters are directly estimated by the difference in detected foot contacts events. Nevertheless, the obtained errors ($3,99\% \leq \epsilon \leq 8,09\%$) have good acceptability, and, therefore, deviations in our system measurements may not be significant. In comparison with the literature, besides, we measured more gait-associated metrics, the percentage of absolute error measured for stride time ($\epsilon = 3,44\%$), step length ($\epsilon = 3,02\%$) and velocity ($\epsilon = 6,41\%$), considering the reference of the trials at a normal velocity, was lower in the present study than in (Fusca et al., 2018) (stride time $\epsilon = 5,7\%$; step length $\epsilon = 5,6\%$; and velocity $\epsilon = 13,5\%$). In fact, the acceptability of the obtained errors leads us to believe that H-GED algorithm can be used to analyze and estimate gait parameters in healthy subjects. This fact boosted us to the system validation in Experiment II, with end users, patients with PD.

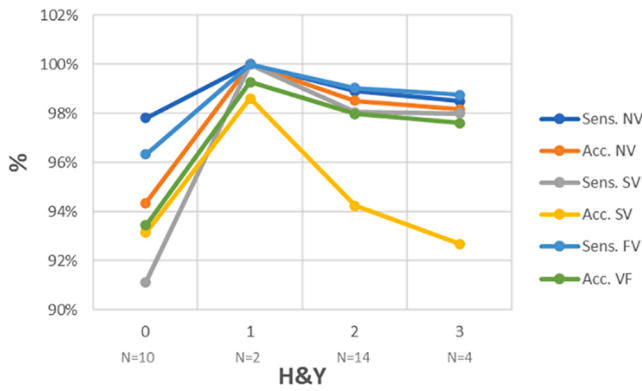


Fig. 11. H-GED and PD-GED algorithm performance, regarding sensitivity (Sens.) and accuracy (Acc.) for the normal (NV), slow (SV) and fast (FV) velocity trials, according to H&Y stage.

5.2. Experiment II

The main goal of the present study was the development of a new gait analysis system for PD, able to segment a gait cycle and estimate gait spatiotemporal parameters. Thus, Experiment II aimed to extend the results obtained in Experiment I but validating with the end-users adaptations introduced in the computational method, with PD patients and at the Hospital of Braga facilities. It aimed to assess the proposed solution through repeated gait measurements of patients with PD (considering three velocities: normal, slow, and fast). Its validation included an analysis on the performance of the gait segmentation algorithm and a benchmarking analysis on the estimation of gait parameters. Further, we performed an analysis from the clinical point of view with the measured gait parameters.

Natural gait patterns observed in healthy adults are altered by PD, which is manifested by altered trunk inertial patterns and consequent compensatory movements. These patients usually walk more slowly than healthy adults, which increases the error in estimated gait events. We realized that the proposed computational method for gait events detection had to be adapted to PD patients (PD-GED), while still maintaining the ability to detect the five walking events and the adaptability and motion compensation features. It was accomplished some adaptations in the FSM decision rules regarding the maximum/minimum peaks detection. The PD-GED is also coupled to a threshold-based structure

where the FSM detects the events and, in parallel, updates the thresholds used in the heuristic decision rules. Besides the adaptive thresholds, the motion compensation strategy was maintained. In addition, it was added a new capability of distinguishing which leg was performing an event without initial assumptions.

PD-GED algorithm showed to be highly sensitive (total mean of 99,53%) and accurate (total mean of 97,42%) for the detection of the proposed events for different walking velocity trials. Additionally, the introduced adaptations did not affect the high temporal algorithm performance, since we observed that the proposed solution proved to be time-effective for real-time gait events detection due to the insignificant values of delay and advances (E: ROME = 0,82%; D: ROME = 0,91%). Advantageously, these metrics were measured for different gait velocities and against a pre-validated IMU-based ground-truth system, contrarily to (Trojaniello et al., 2015). Trojaniello et al., 2015 obtained a good algorithm performance for a protocol which included free walk along a 12 m walkway without addressing different gait speeds. Further, it only focused HS and TO events detection, while our solution can segment a complete gait cycle into all five gait events. The quality of PD-GED performance is also due to the adopted features of adaptability and motion compensation. In fact, we found that these features were vital for the detection of gait events accurately and efficiently, regardless of the test velocities and the character of intra-variability of the participants. However, it is noteworthy that despite the promising results, future work should address the validation of the system with other motors tasks and in home scenarios.

Similarly to the outcomes from Experiment I and aligned with the observations in (González et al., 2010; McCamley et al., 2012; Zijlstra & Hof, 2003), the performance of the computational method is most affected for slower gait velocities trials (SV: $\bar{x} \pm SD = 0,71 \pm 0,06$ m/s), since it is observed a less fluid gait. This common observation leads us to believe that, in the future, a calibration phase should be added to the proposed procedure. Previously to using the system, the user would travel a fixed distance at a slow, normal, and fast speed, while the maximum and minimum acceleration peaks are collected and used to adapt the adaptive thresholds and events range duration to the users' gait. This is expected to greatly improve the performance of the proposed algorithms for gait event detection and consequent gait parameters estimation. Furthermore, we believe that this new routine will help to improve the PD-GED algorithm performance for patients in an evolved disease state.

The proposed gait analysis systems besides to provide gait events

Table 9

Benchmarking analysis of gait parameters estimation. Percentage of absolute error ($\epsilon\%$) measured from the obtained gait parameters for the different walking trials (vV_x) and as a mean ($\bar{x} \epsilon\%$) for each trial (NV_x , SV_x and FV_x), and trial velocity mean \pm standard deviation. Reliability assessment by colors: green – excellent ($\epsilon\% < 5\%$); blue – good ($5\% \leq \epsilon\% < 10\%$); yellow – sufficient ($10\% \leq \epsilon\% < 20\%$); red – not acceptable ($\epsilon\% \geq 20\%$).

Trial	Step Duration $\epsilon\%$	Stride Duration $\epsilon\%$	Step Length $\epsilon\%$	Stride Length $\epsilon\%$	Velocity $\epsilon\%$	Cadence $\epsilon\%$	Trial Velocity [m/s] ($\bar{x} \pm SD$)
NV1	5,72	4,15	5,64	4,15	8,48	4,94	0,82±0,02
NV2	1,13	1,77	9,08	4,54	10,98	13,51	
NV3	10,50	2,50	7,12	2,21	7,97	7,88	
$\bar{x} \epsilon\%$	8,37	2,81	7,28	3,68	9,14	8,78,	
SV1	3,96	3,77	12,17	6,98	9,58	9,55	0,71±0,06
SV2	8,88	5,20	17,29	5,85	15,93	5,82	
SV3	2,01	4,97	10,88	4,02	11,85	3,07	
$\bar{x} \epsilon\%$	4,95	4,65	13,45	5,62	12,45	6,14	
FV1	12,08	10,25	18,10	17,64	5,52	9,15	0,93±0,006
FV2	3,45	3,20	8,08	3,21	6,99	3,52	
FV3	4,22	1,18	8,48	1,78	6,69	3,77	
$\bar{x} \epsilon\%$	6,58	4,88	11,55	7,54	6,40	5,48	

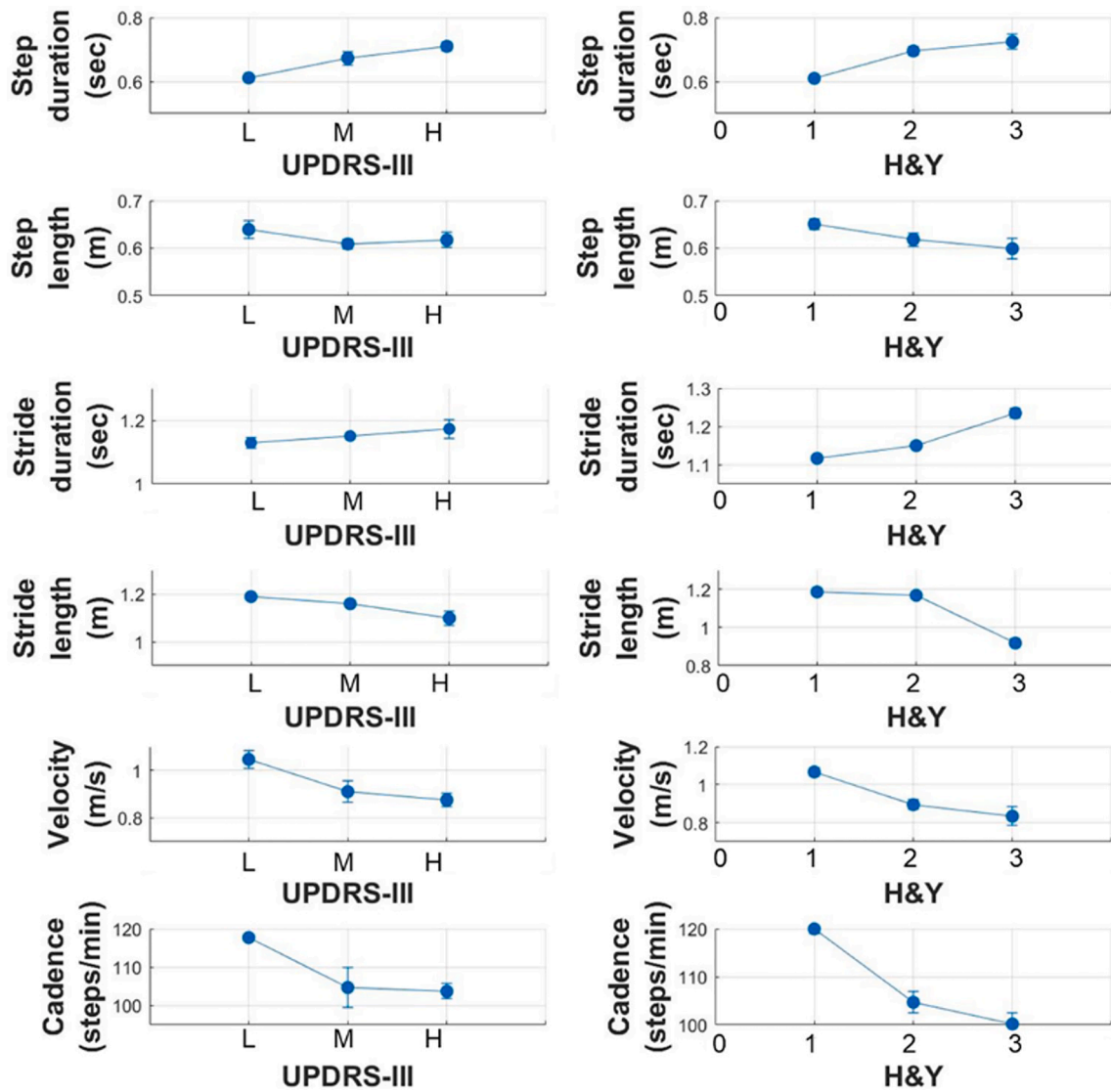


Fig. 12. Measured group gait spatiotemporal parameters of PD patients (cross-sectional study). Step/stride duration/length, velocity and cadence were calculated for PD patients grouped according to UPDRS-III total score (left) and H&Y disease stage (right). Group data are displayed as mean \pm SEM.

detection, it is capable to measure six gait spatiotemporal parameters (step/stride duration/length, velocity, and cadence) with a good error ($2,81\% \leq \epsilon \leq 4,88\%$) for different gait velocities. We identified two possible causes for some error deviations. First, wearable systems must be properly and firmly attached to the human body to avoid vibration artifacts in IMU measurements, which cannot be removed by filtering since they are in the signals' frequency band. A second aspect that can contribute to the measurement errors, is that a bad alignment of the measuring devices can also introduce deviations in the systems' measurements. To circumvent these sources of error, it was always the same person who placed the sensors in the participants' body, and it was used anatomical references for their arrangement in the body segments to guarantee a uniform placement. In the mean term, dynamic calibration procedures to compensate these misalignments are being addressed. Nevertheless, the measured percentages of absolute error were classified as acceptable for gait parameters estimation. Indeed, the adaptive and accurate gait events detection and the ability of estimating six gait parameters with low error, means that the developed system has the potential to be used as a gait monitoring system in PD. Thus, it is expected that the system can be used during gait monitoring sessions (domiciliary/rehabilitation/assistance context) or during routine consultations, to provide continuous, quantitative, and objective information of

patients' gait to clinicians.

A continuous gait parameters assessment correlated with disease-associated clinical scales, may determine that, in the future, the assessment of gait spatiotemporal metrics will constitute a biomarker of the disease stage, allowing to obtain a more personalized treatment (Pistacchi et al., 2017). As expected for a characteristic *parkinsonian* gait, patients with increased motor severity (UPDRS-III) and advance disease stage (H&Y) presented longer step/stride duration, smaller step/stride length, slower velocity and cadence (Perlmutter, 2009; Pistacchi et al., 2017). These results are still preliminary to conclude the hypothesis that based on the assessment of patients' motor function, it will be possible to "bio-mark" the patient's stage given that it is required a larger sample population to better characterize each group-stage of the disease and a more critical statistical analysis. However, we observed that the proposed solution is able to evaluate the PD prototypical gait-associated metrics, besides to contribute with a system able to estimate more gait spatiotemporal metrics (Schlachetzki et al., 2017). Through the study dissemination to a more representative group, we might obtain a new system that can be used by clinicians, not only to monitor their patients but to contribute as a tool to support clinical decision and in the future serve as a biomarker of the disease stage.

6. Strengths and limitations

- (i) modularity. The proposed solution is easily integrated with other systems, which enable to synchronously accomplish a benchmarking assessment against pre-validated ground-truth systems, allowing to accomplish more reliable experimental protocols for validation. Combining this aspect with the real-time computational method performance, it is possible to integrate our solution with an actuation unit and provide a biofeedback system. This enables to provide on-going assistive techniques while monitoring the user gait.
- (ii) wearability and robustness. The fully integration of the electronic components in a robust waistband enabled to achieve non-intrusive and easily hidden system under users' clothes. The instrumented device is adjustable for different physiognomies and enables a continuous assessment, which is required for application in home scenarios with longer times of acquisition.
- (iii) intra-/inter-user versatility. The heuristic decision rules included in the proposed FSM involve the inertial lower trunk information that varies with gait speed and motor tasks. Consequently, the algorithm's adaptability proved to be a key feature for the successful application of the proposed gait event detection system in real-life situations, and it enabled the algorithm to handle intra-/inter-step variability. This feature makes this computational method a potential benchmark approach for real-time human gait segmentation. Moreover, the proposed experimental protocols included different walking tasks and gait speeds for the validation of the proposed technology.

However, there are still some limitations. First, although sensors were carefully positioned on the participants' bodies, their precise positioning is affected by the participants' anatomy as well as by gender and age. This may have led to possible differences in terms of algorithm performance. Second, it is imperative to validate our wearable technology in home scenarios and include other walking tasks in experimental protocols to assess our solution capabilities to promote users' freedom of movement. Third, it is required more clinical evidence, evaluate the device usability level, and validate the system with matched adults' participants. Further, it was measured six gait spatiotemporal parameters, but additional gait parameters can be assessed, as stance/swing time. Lastly, it is necessary to extend the gait parameters vs clinical scales analysis to a more representative sample and framed on longitudinal clinical study.

7. Conclusions

Making use of recent wearable technology, it was developed a new gait monitoring system adapted to PD, able to provide objective and feasible patients' walking information. The effectiveness of the proposed system gait events detection and gait spatiotemporal estimation was assessed. The proposed real-time gait event detection system has shown to be accurate, time-effective, user-adaptable, user-motion compensated, low-cost, with a low computational cost for gait analysis. It has proven its power of portability and wearability, since it has been used in different environments and by different participants. Also, it was verified that the adaptability introduced in the gait events detection enables accurate gait analysis for different walking conditions and may guarantee more robustness for sporadic perturbations. These features make the system suitable to be used as a gait assessment tool or be integrated on rehabilitation/assistance devices. Furthermore, combining these aspects with the ability of the system to estimate gait spatiotemporal parameters, makes this system suitable as a quantitative benchmark of human locomotion.

Future challenges include to (i) implement a longitudinal study, (ii) increase the clinical evidence, (iii) involve more walking tasks on the protocol and (iv) establish clinical correlations with gait spatiotemporal

parameters from patients in different disease stages and over the time. Moreover, as a challenge, we will integrate the proposed system with an actuation tool for assistance/rehabilitation purpose in PD, given the real-time and durability qualities. Lastly, machine learning techniques can also be explored to investigate the ability of IMU-based gait analysis to discriminate patients with PD at different severity stages from age-matched healthy individuals.

Declaration of Competing Interest

The authors declare that they have no known competing financial interests or personal relationships that could have appeared to influence the work reported in this paper.

Acknowledgements

This work was supported by FCT national funds, under the national support to R&D units grant, through the reference project UIDB/04436/2020 and UIDP/04436/2020, and under the Reference Scholarship under grant SFRH/BD/136569/2018.

References

- Alvarez, J. C., Lo, A. M., Rodriguez-uri, J., Diego, A., & Gonza, R. C. (2010). Real-time gait event detection for normal subjects from lower trunk. *Gait and Posture*, 31, 322–325. <https://doi.org/10.1016/j.gaitpost.2009.11.014>
- Auvinet, B., Berrut, G., Touzard, C., Moutel, L., Collet, N., Chaleil, D., & Barrey, E. (2002). Reference data for normal subjects obtained with an accelerometric device. *Gait and Posture*, 16(2), 124–134. [https://doi.org/10.1016/S0966-6362\(01\)00203-X](https://doi.org/10.1016/S0966-6362(01)00203-X)
- Beck, Y., Herman, T., Brozgol, M., Giladi, N., Mirelman, A., & Hausdorff, J. M. (2018). SPARC: A new approach to quantifying gait smoothness in patients with Parkinson's disease. *Journal of NeuroEngineering and Rehabilitation*, 15(1), 1–9. <https://doi.org/10.1186/s12984-018-0398-3>
- Brogna, L., Palumbo, P., Grimm, B., & Palmerini, L. (2019). Assessing Gait in Parkinson's Disease Using Wearable Motion Sensors: A Systematic Review. *Diseases*, 7(1), 18. <https://doi.org/10.3390/diseases7010018>
- Caramia, C., Torricelli, D., Schmid, M., Munoz-Gonzalez, A., Gonzalez-Vargas, J., Grandas, F., & Pons, J. L. (2018). IMU-Based Classification of Parkinson's Disease from Gait: A Sensitivity Analysis on Sensor Location and Feature Selection. *IEEE Journal of Biomedical and Health Informatics*, 22(6), 1765–1774. <https://doi.org/10.1109/JBHI.2018.2865218>
- Del Din, S., Hickey, A., Ladha, C., Stuart, S., Bourke, A. K., Esser, P., Rochester, L., & Godfrey, A. (2016). Instrumented gait assessment with a single wearable: an introductory tutorial. *F1000Research*, 5(May), 2323. DOI:10.12688/f1000research.9591.1.
- Del Din, S., Godfrey, A., Galna, B., Lord, S., & Rochester, L. (2016). Free-living gait characteristics in ageing and Parkinson's disease: Impact of environment and ambulatory bout length. *Journal of NeuroEngineering and Rehabilitation*, 13(1), 1–12. <https://doi.org/10.1186/s12984-016-0154-5>
- Del Din, S., Godfrey, A., & Rochester, L. (2016). Validation of an accelerometer to quantify a comprehensive battery of gait characteristics in healthy older adults and Parkinson's disease: Toward clinical and at home use. *IEEE Journal of Biomedical and Health Informatics*, 20(3), 838–847. <https://doi.org/10.1109/JBHI.2015.2419317>
- Dijkstra, B., Zijlstra, W., Scherder, E., & Kamsma, Y. (2008). Detection of walking periods and number of steps in older adults and patients with Parkinson's disease: Accuracy of a pedometer and an accelerometry-based method. *Age and Ageing*, 37(4), 436–441. <https://doi.org/10.1093/ageing/afn097>
- Ferdinando, H., Khoswanto, H., & Purwanto, D. (2012). Embedded Kalman filter for inertial measurement unit (IMU) on the ATmega8535. INISTA 2012 - International Symposium on INnovations in Intelligent Systems and Applications, October 2014. DOI:10.1109/INISTA.2012.6246978.
- Figueiredo, J., Felix, P., Costa, L., Moreno, J. C., & Santos, C. P. (2018). Gait event detection in controlled and real-life situations: Repeated measures from healthy subjects. *IEEE Transactions on Neural Systems and Rehabilitation Engineering*, 26(10), 1945–1956. <https://doi.org/10.1109/TNSRE.733310.1109/TNSRE.2018.2868094>
- Fusca, M., Negrini, F., Perego, P., Magoni, L., Molteni, F., & Andreoni, G. (2018). Validation of a wearable IMU system for gait analysis: Protocol and application to a new system. *Applied Sciences (Switzerland)*, 8(7), 1–16. <https://doi.org/10.3390/app8071167>
- Godinho, C., Domingos, J., Cunha, G., Santos, A. T., Fernandes, R. M., Abreu, D., ... Ferreira, J. J. (2016). A systematic review of the characteristics and validity of monitoring technologies to assess Parkinson's disease. *Journal of NeuroEngineering and Rehabilitation*, 13(1), 1–10. <https://doi.org/10.1186/s12984-016-0136-7>
- Goetz, C. G., Tilley, B. C., Shaftman, S. R., Stebbins, G. T., Fahn, S., Martinez-Martin, P., ... LaPelle, N. (2008). Movement Disorder Society-Sponsored Revision of the Unified Parkinson's Disease Rating Scale (MDS-UPDRS): Scale presentation and clinimetric testing results. *Movement Disorders*, 23(15), 2129–2170. <https://doi.org/10.1002/mds.22340>

- Gonçalves, H. R., Moreira, R., Rodrigues, A., Minas, G., Reis, L. P., & Santos, C. P. (2018). Real-time tool for human gait detection from lower trunk acceleration. In *Advances in Intelligent Systems and Computing* (Vol. 747). DOI:10.1007/978-3-319-77700-9_2.
- González, R. C., López, A. M., Rodríguez-Uría, J., Álvarez, D., & Alvarez, J. C. (2010). Real-time gait event detection for normal subjects from lower trunk accelerations. *Gait and Posture*, 31(3), 322–325. <https://doi.org/10.1016/j.gaitpost.2009.11.014>
- Hoehn, M. M., & Yahr, M. D. (1967). Parkinsonism: Onset, progression, and mortality. *Neurology*, 17(May). <https://doi.org/10.1212/WNL.17.5.427>
- Hundza, S. R., Hook, W. R., Harris, C. R., Mahajan, S. V., Leslie, P. A., Spani, C. A., ... Livingston, N. J. (2014). Accurate and reliable gait cycle detection in parkinson's disease. *IEEE Transactions on Neural Systems and Rehabilitation Engineering*, 22(1), 127–137. <https://doi.org/10.1109/TNSRE.2013.2282080>
- Iijima, H., & Takahashi, M. (2020). State of the Field of waist-mounted sensor algorithm for gait events detection: A scoping review. *Gait and Posture*, 79(March), 152–161. <https://doi.org/10.1016/j.gaitpost.2020.03.021>
- Jakobsen, J. C., Gluud, C., Winkel, P., Lange, T., & Wetterslev, J. (2014). The thresholds for statistical and clinical significance - A five-step procedure for evaluation of intervention effects in randomised clinical trials. *BMC Medical Research Methodology*, 14(1), 1–12. <https://doi.org/10.1186/1471-2288-14-34>
- Linares-del Rey, M., Vela-Desojo, L., & Cano-de la Cuerda, R. (2019). Mobile phone applications in Parkinson's disease: A systematic review. *Neurología (English Edition)*, 34(1), 38–54. <https://doi.org/10.1016/j.nrleng.2018.12.002>
- Link, C., Patel, S., Lorincz, K., Hughes, R., Huggins, N., Growdon, J., ... Member, S. (2009). Monitoring motor fluctuations in patients with Parkinson's disease using wearable sensors. *IEEE Transactions on Information Technology in Biomedicine*, 13(6), 864–873. <https://doi.org/10.1109/TITB.2009.2033471>
- Lipsmeier, F., Taylor, K. I., Kilchenmann, T., Wolf, D., Scotland, A., Schjodt-Eriksen, J., ... Lindemann, M. (2018). Evaluation of smartphone-based testing to generate exploratory outcome measures in a phase 1 Parkinson's disease clinical trial. *Movement Disorders*, 33(8), 1287–1297. <https://doi.org/10.1002/mds.27376>
- Maetzler, W., Domingos, J., Srulijes, K., Ferreira, J. J., & Bloem, B. R. (2013). Quantitative wearable sensors for objective assessment of Parkinson's disease. *Movement Disorders*, 28(12), 1628–1637. <https://doi.org/10.1002/mds.25628>
- McCarmley, J., Donati, M., Grimpampi, E., & Mazzà, C. (2012). An enhanced estimate of initial contact and final contact instants of time using lower trunk inertial sensor data. *Gait and Posture*, 36(2), 316–318. <https://doi.org/10.1016/j.gaitpost.2012.02.019>
- Mccarron, B. (2013). Low-Cost IMU Implementation via Sensor Fusion Algorithms in the Arduino Environment. California Polytechnic State University, June.
- Menz, H. B., Lord, S. R., & Fitzpatrick, R. C. (2003). Acceleration patterns of the head and pelvis when walking on level and irregular surfaces. *Gait and Posture*, 18(1), 35–46.
- Moore, S. T., Dilda, V., Hakim, B., & MacDougall, H. G. (2011). Validation of 24-hour ambulatory gait assessment in Parkinson's disease with simultaneous video observation. *BioMedical Engineering Online*, 10(1), 82. <https://doi.org/10.1186/1475-925X-10-82>
- Morris, R., Stuart, S., McBarron, G., Fino, P. C., Mancini, M., & Curtze, C. (2019). Validity of mobility lab (version 2) for gait assessment in young adults, older adults and Parkinson's disease. *Physiological Measurement*, 40(9), 095003. <https://doi.org/10.1088/1361-6579/ab4023>
- Okuda, S., Takano, S., Ueno, M., Hara, Y., Chida, Y., Ikkaku, T., Kanda, F., & Toda, T. (2016). Gait analysis of patients with Parkinson's disease using a portable triaxial accelerometer. *Neurology and Clinical Neuroscience*, 4(3), 93–97. <https://doi.org/10.1111/ncn3.12043>
- Palacios-Alonso, D., Melendez-Morales, G., Lopez-Arribas, A., Lazaro-Carrascosa, C., Gomez-Rodellar, A., & Gomez-Vilda, P. (2020). MonParLoc: A Speech-Based System for Parkinson's Disease Analysis and Monitoring. *IEEE Access*, 8, 188243–188255. <https://doi.org/10.1109/Access.628763910.1109/ACCESS.2020.3031646>
- Patel, S., Lorincz, K., Hughes, R., Huggins, N., Growdon, J. H., Welsh, M., & Bonato, P. (2007). Analysis of feature space for monitoring persons with Parkinson's disease with application to a wireless wearable sensor system. In *Annual International Conference of the IEEE Engineering in Medicine and Biology - Proceedings* (pp. 6290–6293). <https://doi.org/10.1109/IEMBS.2007.4353793>
- Perlmutter, J. S. (2009). Assessment of Parkinson disease manifestations. *Current Protocols in Neuroscience*, (SUPPL.49), 1–16. <https://doi.org/10.1002/0471142301.nsl001s49>
- Pistacchi, M., Gioulis, M., Sanson, F., de Giovannini, E., Filippi, G., Rossetto, F., & Marsala, S. Z. (2017a). Gait analysis and clinical correlations in early Parkinson's disease. *Functional Neurology*, 32(1), 28–34. DOI:10.11138/FNeur/2017.32.1.028.
- Rastegari, E., Azizian, S., & Ali, H. (2019). Machine Learning and Similarity Network Approaches to Support Automatic Classification of Parkinson's Diseases Using Accelerometer-based Gait Analysis. Proceedings of the 52nd Hawaii International Conference on System Sciences, 6, 4231–4242. DOI:10.24251/hicss.2019.511.
- Schlachetzk, J. C. M., Barth, J., Marxreiter, F., Gossler, J., Kohl, Z., Reinfelder, S., ... Klucken, J. (2017). Wearable sensors objectively measure gait parameters in Parkinson's disease. *PLoS ONE*, 12(10), 1–18. DOI:10.1371/journal.pone.0183989.
- Suzuki, M., Mitoma, H., & Yoneyama, M. (2017). Quantitative analysis of motor status in Parkinson's disease using wearable devices: From methodological considerations to problems in clinical applications. *Parkinson's Disease*, 2017, 1–9. <https://doi.org/10.1155/2017/6139716>
- Sweeney, D., Quinlan, L., Browne, P., Richardson, M., Meskell, P., & ÓLaighin, G. (2019). A technological review of wearable cueing devices addressing freezing of gait in Parkinson's disease. *Sensors (Switzerland)*, 19(6), 1277. <https://doi.org/10.3390/s19061277>
- Technologies, X. (2018). Xsens MVN. User Guide Xsens MVN, MVN Link, MVN Awinda, October.
- Trojaniello, D., Cereatti, A., Pelosin, E., Avanzino, L., Mirelman, A., Hausdorff, J. M., & Della Croce, U. (2014). Estimation of step-by-step spatio-temporal parameters of normal and impaired gait using shank-mounted magneto-inertial sensors. *Journal of NeuroEngineering and Rehabilitation*, 1–12. <https://doi.org/10.1016/j.jdent.2015.05.012>
- Trojaniello, D., Ravaschio, A., Hausdorff, J. M., & Cereatti, A. (2015). Comparative assessment of different methods for the estimation of gait temporal parameters using a single inertial sensor: Application to elderly, post-stroke, Parkinson's disease and Huntington's disease subjects. *Gait and Posture*, 42(3), 310–316. <https://doi.org/10.1016/j.gaitpost.2015.06.008>
- Vicon. (2010). Vicon Nexus User Interface.
- Windau, J., & Itti, L. (2016). Walking compass with head-mounted IMU sensor. Proceedings - IEEE International Conference on Robotics and Automation, 2016-June, 5542–5547. DOI:10.1109/ICRA.2016.7487770.
- Windau, J., & Itti, L. (2013). Situation awareness via sensor-equipped eyeglasses. *IEEE International Conference on Intelligent Robots and Systems*, 5674–5679. <https://doi.org/10.1109/IRoS.2013.6697178>
- Zago, M., Sforza, C., Pacifici, I., Cimolin, V., Camerota, F., Celletti, C., Condoluci, C., De Pandis, M. F., & Galli, M. (2018). Gait evaluation using inertial measurement units in subjects with Parkinson's disease. *Journal of Electromyography and Kinesiology*, 42 (June), 44–48. <https://doi.org/10.1016/j.jelekin.2018.06.009>
- Zijlstra, W., & Hof, A. L. (2003). Assessment of spatio-temporal gait parameters from trunk accelerations during human walking. *Gait and Posture*, 18(2), 1–10.